FACILITY FORM 602

N66-18311
(ACCESSION NUMBER)

(THRU)

53
(PAGES)

1
(CODE)

CR-54486
(NASA CR OR TMX OR AD NUMBER)

17
(CATEGORY)

NASA CR-54486

GPO PRICE $ _____

CFSTI PRICE(S) $ _____

Hard copy (HC) 3.00

Microfiche (MF) .50

ff 653 July 65

SEMI-ANNUAL REPORT NO. 1

DEVELOPMENT OF HIGH-TEMPERATURE CHROMIUM ALLOYS

by

J.W. CLARK and C.S. WUKUSICK

prepared for

NATIONAL AERONAUTICS AND SPACE ADMINISTRATION

Contract NAS3-7260

MATERIALS DEVELOPMENT LABORATORY

GENERAL ELECTRIC

FLIGHT PROPULSION DIVISION

NOTICE

This report was prepared as an account of Government sponsored work. Neither the United States, nor the National Aeronautics and Space Administration (NASA), nor any person acting on behalf of NASA:

A.) Makes any warranty or representation, expressed or implied, with respect to the accuracy, completeness, or usefulness of the information contained in this report, or that the use of any information, apparatus, method, or process disclosed in this report may not infringe privately owned rights; or

B.) Assumes any liabilities with respect to the use of, or for damages resulting from the use of any information, apparatus, method or process disclosed in this report.

As used above, "person acting on behalf of NASA" includes any employee or contractor of NASA, or employee of such contractor, to the extent that such employee or contractor of NASA, or employee of such contractor prepares, disseminates, or provides access to, any information pursuant to his employment or contract with NASA, or his employment with such contractor.

NASA CR-54486

SEMI-ANNUAL REPORT NO. 1

DEVELOPMENT OF HIGH-TEMPERATURE CHROMIUM ALLOYS

by

J. W. Clark and C. S. Wukusick

Prepared for

NATIONAL AERONAUTICS AND SPACE ADMINISTRATION

OCTOBER 25, 1965

CONTRACT NAS 3-7260

Technical Management
NASA Lewis Research Center
Cleveland, Ohio
John P. Merutka, Project Manager
William D. Klopp, Research Advisor

GENERAL ELECTRIC COMPANY
Cincinnati, Ohio 45215

DEVELOPMENT OF HIGH-TEMPERATURE CHROMIUM ALLOYS

by J. W. Clark and C. S. Wukusick

General Electric Company

N66-18311

SUMMARY

Chromium alloys which represent several separate approaches are being prepared by induction melting of moderate sized heats and by arc melting of small buttons and drop castings. Gross oxygen contamination which occurred in the first group of induction-melted alloys has been corrected by revisions in the consolidation technique, and alloys with total gaseous impurity levels below 150 ppm are currently being produced by induction melting.

Cold workability was demonstrated in chill cast alloys in the Cr-Re-Co and Cr-Ru-Co systems at Re and Ru levels as low as 11 and 8.5 atomic percent, respectively. Dilute alloys of Cr-Y with dispersions of ZrC and HfC exhibited bend ductility at or below room temperature and retained ductile-brittle transition temperatures of 200° to 400°F after 100-hour air oxidation at 2100°F. Initial results indicated that additions of La and Pr are even more effective than Y in preventing nitridation during air exposure, particularly at 2400°F.

Author

INTRODUCTION

This is the first semi-annual report of work performed on a 24-month chromium alloy development program, which is being conducted jointly by the Materials Development Laboratory and the Nuclear Materials and Propulsion Operation of General Electric. The over-all objective of the program is to identify chromium-base alloys for application in critical parts in high performance air-breathing engines. The desired properties of the resultant alloys, namely:

1. Stress-rupture strength of 15,000 psi at 2100°F/3000 hours (blades),
2. Stress-rupture strength of 4,000 psi at 2400°F/3000 hours (vanes),
3. A notch-impact transition temperature of 80° to 300°F as fabricated;

presently extremely challenging targets. Although it is possible that a Cr alloy with any one of these properties can be identified, it is not considered likely that the strength and notch-impact targets can be combined in a single alloy based on present technology. However, studies over the past several years indicate that additional advances in Cr are highly probable and should be pursued. With this in mind, the present program was undertaken with the objective of extending the useful time/temperature/stress conditions under which Cr alloys can be applied in advanced air breathing engines through alloying approaches designed to improve strength, ductility, and nitridation resistance.

Several significant advances have been made in the technology of Cr alloys over the past several years. The addition of reactive elements such as yttrium was found to improve the resistance to nitrogen absorption. The mechanism(s) by which reactive-metal additions improve the resistance to nitridation have not been completely defined, but the effect has been well documented and is reproducible. Combinations of Y with other reactive metal additions such as Th and Hf are more effective than single additions in improving both nitridation resistance and retention of ductility after high-temperature exposure. An alloy of Cr-Y-Th-Hf, where the total alloy content was less than 0.5 wt. percent, was resistant to nitridation for 100 hours at 2300°F in thin (0.022 inch) sections. There was no evidence of incipient melting and the ductile-brittle transition temperature (DBTT) in bending was about 300°F in the as-oxidized condition.

As a result of the improvement afforded by small amounts of Y, the Cr-Y system has been used as a base for several alloy development programs. It has made possible the induction melting process for primary consolidation and permitted use of Cr of only moderate purity. The resultant alloy purity was in most cases comparable to that produced by arc melting of high purity Cr. The melting process consisted of melting hydrogen-reduced electrolytic flake in a Y_2O_3-stabilized ZrO_2 crucible in an inert atmosphere. Y was added to getter interstitial impurities from the melt and to provide a slight excess in the alloy for subsequent oxidation-nitridation resistance. The cost of the H_2-reduced flake is one-fourth to one-third the cost of crystals produced by the iodide process.

The addition of Groups VII and VIII metals to Cr in some cases results in a striking improvement in low temperature ductility. The Cr-65 w/o Re alloy is analogous to W-25Re and Mo-50Re alloys. Recently, Cr-Ru alloys were found to exhibit excellent ductility in both the recrystallized condition and after 120-hour oxidation at 2000°F. However, like Re, large amounts ($\sim$ 30%) of Ru are required to provide a high degree of ductility. A further disadvantage of Ru is a decrease in melting point to about 2900°F for a Cr-30 Ru alloy compared to a melting point of about 4000°F in Cr-65Re. To date, the only relatively inexpensive metal which when added to Cr in moderate amounts causes ductility improvements similar to Re, is Co. Single phase alloys containing 25 to 35% Co prepared by chill casting have exhibited considerable plasticity in room temperature rolling experiments.

Since the equilibrium solubility of Co in Cr is only about 10% at 1800°F, the alloys were supersaturated in the chill-casting process. It is clear that practical binary Cr-Co alloys will not be developed, since the terminal solubility drops rapidly with temperature. It is possible, however, that substitution of Co for part of the Re (or Ru) in ternary Cr base alloys could result in useful materials.

The Cr-65Re alloy probably represents the best combination of strength and ductility in a Cr-base alloy available at the present time. Estimates based on hot hardness data indicate that at 2100°F the ultimate tensile strength is about 90,000 psi and at 2400°F is about 60,000 psi.

One of the most significant developments in Cr alloy technology has been the improvements in strength and ductility afforded by carbide dispersions. Fine carbide dispersions have been shown to result in increased high-temperature strength while simultaneously increasing low-temperature ductility. It is reasoned that the carbide particles act as sinks for other interstitials, particularly nitrogen, thereby improving ductility. Stress rupture strengths of representative alloys are shown in Figure 1, with unalloyed Cr data included for comparison. Tensile properties of several alloys are compared in Table 1. Based on early data, the lower-C alloys with Zr or Hf-rich reactive metal additions were clearly superior to higher-C alloys. The normal structure of this type of alloy contained ZrC and (Zr, Ti) (C,N) phases of the NaCl type. Heat treatment at 2000-2250°F dissolved non-equilibrium $Cr_{23}C_6$ present in as-worked structures, and precipitated dissolved interstitials as (Ti,Zr) (C,N) and/or ZrN. This removal of interstitials from solution, especially nitrogen, produced excellent ductility with DBTT values as low as -50°F. The low DBTT values could be retained even when the alloy was contaminated by 900-1000 ppm oxygen + nitrogen, provided that a sufficient reactive metal concentration was maintained to getter the contaminants.

The combination of solid-solution and carbide dispersion mechanisms resulted in further advances in Cr-base alloys. Figure 2 summarizes the stress rupture properties of several alloys. The addition of W to a carbide strengthened alloy resulted in significant strength increases. The C-207 alloy represents the best combination of strength, ductility, and oxidation resistance of any known Cr-base alloy except perhaps the Cr-65 Re alloy. The C-207 alloy has been prepared as 100-pound induction melted heats and its properties have been extensively investigated. It also has been successfully forged into turbine blades. Figure 3 shows tensile data from the heat employed in forging.

Utilizing the above background as a starting point, the present program was undertaken to further develop the potential of Cr-base alloys for use in advanced air-breathing engines.

PROGRAM ORGANIZATION

The experimental program is divided into Task I and Task II. Task I, which comprises the first 15 months of the program,consists of evaluation of some 60 to 65 alloys to be melted from charges of four pounds each. Also included in Task I are several groups of alloys prepared as buttons of 50 to 100 grams. Several of the four-pound heats in the later phases of Task I will be selected from the button alloys after evaluation of the latter for specific properties.

Upon completion of Task I, the five alloys with the most useful combination of strength, ductility, and oxidation resistance will be selected for preparation as approximately 14-pound heats. These alloys will be evaluated in much greater detail than in Task I. Since Task II alloy selection is in the future, the remainder of this report is concerned only with Task I.

ALLOY DESIGN

In order to provide improvements in strength, ductility and oxidation-nitridation resistance, five broad classes of alloys are included in the study. These five types of alloy systems, with examples of the additions being made, are:

1. Nitridation inhibitors (Y, Th, Hf)
2. Solid-solution strengtheners (Mo, W, V)
3. Solid-solution ductilizers (Re, Ru, Co)
4. Dispersion strengtheners (carbides, borides, intermetallics)
5. Complex combinations of above.

In several instances, sufficient data are available from prior work to specify compositions which merit full evaluation in Task I. In other cases, this prior work has identified potentially fruitful alloying approaches, but has not proceeded to the point that exact compositions can be recommended with confidence. In the latter instances, it was considered more efficient to first conduct surveys of such alloy systems using heats of smaller size and confining the evaluation to the most critical characteristic(s) affected by the variable under study. This approach was adopted for this program, and four separate phases of alloy design are being undertaken in Task I:

A. First series of induction-melted heats (3-4 pounds).
B. Small heats for system surveys (50-100 grams).
C. Series of induction-melted heats based on B.
D. Optimized compositions based on A through C.

Two somewhat arbitrary "standards" are employed in the initial phases of Task I. Briefly, the intent is to evaluate several alloying approaches using additions to or departures from the standard alloys. This standard could have been selected as unalloyed Cr or perhaps Cr-Y. Results from either of these would probably yield the same relative rating of the effectiveness of the further additions. The results would not, however, be likely to approach those required for the time/temperature/stress regime of interest here.

The standard solution-strengthened matrix, in atomic percent, is:
Cr-4Mo-.1Y (Cr-7.1Mo-.17Y in weight percent)

One of the basic guidelines in alloy design for high-temperature strength is, of course, the melting point, and the interrelated aspects of atomic mobility and attendant effects on creep. Although other factors such as differences in atomic size and elastic constants are also important, the melting characteristics assume added significance as the time/temperature conditions for stressed service are increased. A review of the effects of Re and other solutes with greater than six orbital electrons was presented in the preceding section. Of the remaining elements with melting points above 3000°F, only W, Mo, and V have extended solubility in Cr. The effects of these solutes on the high-temperature tensile strength of Cr alloys are compared on the following page for concentrations of 3 to 6 atomic percent:

	Average Increase in Tensile Strength (psi/atom %)	
Solute	2000°F	2200°F
V	900	---
Mo	5700	4000
W	9900	8100

As might be expected, W has a considerably higher strengthening effect at these temperatures on an atomic basis. When the increase in strength per weight percent solute is considered, W and Mo are essentially equivalent at 2000°F and W is superior at the higher temperature. However, prior experience in these laboratories indicates that W additions are limited to about 4 atom percent by the solid-state miscibility gap in the Cr-W system. More highly alloyed compositions reject a W-rich solid solution upon aging at temperatures below 1800°F and attempts to work such alloys have not been successful. Alloys with somewhat higher atomic concentrations of Mo have been reduced from ingot to bar stock and their strengths follow the trends shown in the tabulation above. Therefore, Mo alloys have been emphasized in preference to W in the initial phases of Task I. The Cr-4Mo-.1Y alloy selected as the standard matrix will provide an increase of some 20,000 psi in the 2000°F tensile strength over that of Cr or Cr-Y, yet should permit processing without undue difficulty.

The standard reactive-metal/carbon alloy, in atomic percent, is:

Cr-.05Y-.4Zr-.2Ti-.4C

(Cr-.085Y-.7Zr-.2Ti-.09C in weight percent)

The use of a Zr-rich combination of Zr and Ti as the carbide-stabilizing addition represents the approach which has yielded the best balance of critical properties in our prior work. Although it is beyond the scope of this report to discuss the prior data in detail, a short review of conclusions is in order. Both Zr and Hf additions to Cr-Y-C alloys result in the formation of massive carbide particles. Although these large particles provide relatively little dispersion strengthening, the air oxidation behavior and resistance to embrittlement of such alloys is superior. Additions of Ta, Cb, and Ti result in precipitation of fine, uniformly dispersed monocarbides with attractive thermal stability. The strengths of these types of alloys are considerably higher than those which form the coarse carbides, but they are severely embrittled by air oxidation. Alloys with carbides based on a combination of Zr and Ti have structural, strength, and oxidation characteristics which are intermediate between the two groups described above and the thermal stability appears to be superior to either type, with little growth of the carbides observed upon 1000-hour exposure at 2000°F. This type of carbide is used as the standard in Phases A and B of Task I. Volume fractions of the dispersed phase, reactive-metal to interstitial ratios, and compositions of the compound-stabilizing elements have been varied with this standard as the basis for comparison. A limited evaluation of borides is also being performed.

Finally, the desired level of retained yttrium is dependent on the type of alloy under consideration. Binary alloys with residual Y levels of 0.3% and higher are quite easy to work and have good oxidation resistance. Additions of substitutionally soluble elements do not appear to reduce the tolerance for Y, particularly in the case of non-reactive solutes. Carbide-strengthened alloys, on the other hand, are hot-short and suffer intermediate-temperature nitridation and consequent embrittlement at Y contents above 0.2% and most considerations indicate that the optimum level may be more nearly 0.1%. Microprobe scans of such alloys in the latter range and emission analyses of extracted phases show a lower solubility of Y and/or a tendency to segregate to the carbides. For these reasons, an intended Y level of .17% (.1 atom %) is used as a standard in the Phase A alloys which do not contain soluble second phases such as carbides, and a lower level of .085% Y (.05 atom %) has been established as the standard in the dispersion-strengthened alloys.

The compositions of the alloys selected for evaluation in Phase A are listed in Table 2. Solute concentrations are shown here in atomic percent to more clearly indicate the rather dilute nature of most of the alloys in this initial phase. It was not considered necessary to investigate concentrations of the major solutes employed here at levels below 4 a/o since the strengthening at such levels would be inadequate in terms of the targets set for this work. With the exception of V, which has a relatively mild effect on hardness and strength, and of Re, which is known to promote excellent mechanical properties at about 35 a/o, it was felt to be inadvisable to include solution-strengthening additions above 8 a/o in this phase because of difficulties in working even more dilute alloys in prior studies.

Several other types of Cr alloys have been shown to offer promise of improvements in one or more of the critical properties alloys. Insufficient data are presently available to justify the specification of exact compositions for full property screening. Consequently, these approaches are being evaluated in the concurrent Phase B by surveys over broader ranges of solute concentration in small button heats from the pertinent alloy systems. A summary of the systems included in Phase B is shown in Table 3.

OUTLINE OF EVALUATION PROCEDURES

As described above, 40 compositions which represent five general types of alloys have been selected for screening in Phase A. Consolidation of these alloys has been performed primarily by induction melting of H_2-reduced chromium and casting as 2 1/8" diameter ingots. The ingots are processed by extrusion of Mo-canned billets followed by swaging to 1/4" to 3/8" diameter. Wrought bar stock from one representative alloy from each of the five types is subjected to:

1. A complete chemical analysis from three locations in the original ingot to document homogeneity.

2. A microstructural study of heat treatment response in the range 1400°F to values in excess of the solvus temperature of dispersed phases.

3. Low-temperature tensile tests in the three most attractive thermal conditions to determine the ductile-brittle transition temperature.

Heat treatment of the remaining alloys in Phase A is based on the above results. All the following are determined on all Phase A alloys:

1. Analysis of wrought bar stock for interstitials and yttrium to insure the combined O_2 plus N_2 content does not exceed 300 ppm total and that the retained Y level is in the intended range.

2. The ductile-brittle transition temperature in tension.

3. Elevated-temperature tensile strength in vacuum (in the range 1900°-2400°F) in one wrought and one fully recrystallized condition.

4. Air oxidation behavior in the range 1500°-2400°F.

5. Metallographic evaluation of the above specimens.

In Phase B, several different alloying approaches are being studied in terms of specific effects on phase relationships, workability and low-temperature ductility, and resistance to nitrogen embrittlement. Consolidation of these compositions is by arc melting of small buttons or drop castings, and critical alloy interactions in each series are being investigated by selective microstructural analyses, oxidation, forging and rolling trials, and bend testing.

Results from Phases A and B will be used as the basis for design of more nearly optimized alloys in later phases of Task I. Approximately 20 compositions will be prepared and evaluated as in Phase A. In addition to the tests described above, 100-hour creep-rupture strengths will be determined at 2100° and 2400°F for those alloys which exhibit the best combination of other critical properties.

EXPERIMENTAL RESULTS - PHASE A

Initial Consolidation

Analyses of the raw materials used in the preparation of the Phase A alloys are shown in Table 4. In alloys of the types which receive major emphasis in this program, prior work has shown that the use of higher-purity grades of chromium offers no advantage in mechanical properties over the hydrogen-purified electrolytic flake employed here.

Four-pound alloy charges were used throughout the induction melting work described below. Total yttrium concentrations of 0.4 to 0.7% were employed, depending on the desired residual level. In each case the chromium, non-reactive solutes such as molybdenum or tungsten, and 0.3% yttrium were blended and cold pressed into cylindrical briquettes. The remainder of the yttrium and all reactive solutes, such as Group IV A and V A metals and carbon, were placed in a charging tray in the furnace for addition to the melt later in the cycle.

All alloys in the initial portion of the program were melted in a 50 KW Stokes vacuum induction furnace, which can accomodate heat sizes up to about 50 pounds. A Y_2O_3-stabilized ZrO_2 crucible was packed inside the induction coil with coarse ZrO_2 grit serving to insulate the crucible from the coil assembly. The crucible, which was used for only one melt and then replaced, was sealed to the assembly and a ZrO_2 pouring spout was attached to the lip by a paste made from fine ZrO_2 powder. After loading the briquetted charge into the crucible, the furnace was evacuated to a pressure of about 10^{-3} torr. At this point, which was scheduled for mid-afternoon, a power input of 1.5 $\pm$ 0.5 KW was applied to the induction coil with the intention of facilitating more complete removal of water vapor and other adsorbed gases. The temperature of the charge reached 1200°-1400°F and was held in this range for approximately one hour. After this intermediate-temperature outgassing treatment, the power to the coil was shut off and the vacuum system continued to operate over night.

Pressure in the furnace chamber was reduced to at least 10^{-4} torr by the practice described above with leak rates, measured just before applying power to the coil, of 6 $\pm$ 2 x 10^{-5} torr per minute. Initial heating was performed under vacuum, until the charge temperature reached 2000°F. Purified argon was then admitted to the chamber to a partial pressure of 650-700mm, and the remainder of the melting cycle was conducted in this inert atmosphere in order to reduce vaporization of the chromium. The power was increased to 15-18 KW until the charge was completely molten, which required 8-10 minutes from the time the argon was introduced. Power input was then reduced to 10-12 KW, resulting in a stable superheat of 100°-150°. After holding the charge molten for 15 minutes under the static atmosphere of argon, the remainder of the yttrium and any other reactive solutes in the particular alloy were added from the charging tray. Each melt was stirred by rapid cycling between power settings of 12 and 20 KW, held for an additional 4-5 minutes, and cast with power on.

Charges were cast into copper molds fit with 2 1/8" diameter CaO-stabilized ZrO_2 mold liners. These ceramic liners are necessary to prevent solidification cracks which occur in all but the most dilute alloys upon casting directly into copper chill molds. If allowed to freeze in such molds with no hot-topping practice, very extensive shrinkage occurs in cast chromium alloys. In order to prevent this severe pipe, each casting was arc hot-topped by use of a retractable tungsten electrode mounted in the top of the furnace. At a potential of 25 $\pm$ 5 volts, an arc current of 500 amps was employed for 30-45 seconds immediately after pouring and then was gradually

reduced to about 50 amps before arc extinction. This procedure resulted in sound, crack-free ingots of 3-4" height with very shallow shrinkage cavities.

As mentioned in a preceding section, chemical analyses of these alloys were obtained after subsequent surface conditioning and processing to bar stock. In this manner, analyses of material from the center portions of the ingots could be obtained without destructive sectioning of the castings prior to working. In addition to conserving material, this sampling procedure was adopted in order to prevent possibly misleading results which might arise from analysis of the extreme top, bottom, or cylindrical surface of the ingot.

Extrusion and Swaging

After grit blasting to remove remnants of the mold liner, each of the ingots was cropped at least 1/4" below the shallow shrinkage cavity by power hack saw. All the ingots were encased in molybdenum cans with an OD of 2.06" prior to extrusion. They were machined from as-cast diameters of 2.2 $\pm$ .1" to billet diameters of 1.9 $\pm$ .05", the exact dimensions being governed by the ID of the molybdenum can. Lids were welded to the cans by the tungsten arc process in a vacuum-purged chamber back-filled with high purity helium, then the cans were evacuated and sealed by electron beam welding.

All of the first group of alloys were extruded from 2 1/8" diameter containers through 3/4" diameter dies. A summary of the extrusion data is presented in Table 5. Heating was performed in an induction unit under a protective atmosphere of argon. The canned billets were soaked for 30 minutes at temperature, then transferred to the container of a 1250 ton hydraulic press (Lowey Hydropress) with handling times of 10 to 15 seconds. Lubricants were powdered glass plus a mixture of necroline and graphite. The tool steel dies were flame sprayed with ZrO_2 to reduce wash and extend their useful lives. Solid graphite back-up blocks were inserted behind the billets to reduce the extent of the extrusion defects in the trailing ends. Inspection of the extruded stock was performed by radiographic and fluorescent penetrant techniques. Other than minor nose bursts and the typical trailing-end defects, no internal flaws were detected.

Several dilute alloys, such as Cr-Y-(Th) and similar compositions with Zr-Ti and Hf-Zr carbides, were included in this first group to be extruded. Sections of each of these alloys were swaged to 0.25" diameter, using final working temperatures in the range 1800° to 2200°F. Other alloys in this group were from solution-strengthened systems which contain from 4 to 8 atomic percent Mo or W. In contrast to the satisfactory workability observed in the dilute alloys, considerable difficulty was experienced in swaging these more highly alloyed compositions. Moderate to severe cracking occurred during early stages of reduction at all working temperatures in the range 2000° to 2500°F. This behavior was not entirely unexpected at solute levels in the range of 8 atomic percent Mo or W, but was not anticipated at the concentration of 4 atomic percent.

Chemical Analyses

Because of the unexpected processing difficulties described above, analyses of the interstitial and yttrium contents of representative alloys in this first group were undertaken. Cast samples were obtained in each case from the lower side of the slice taken from the top of the ingot prior to canning. Results are shown in Table 6.

Each alloy is highly contaminated by oxygen and essentially all of the yttrium has been lost during melting. The alloys which contain carbon and reactive metals from Group IV A have considerably lower oxygen levels but they are still far above the acceptable limit.

Revised Melting Practice

As a result of the gross oxygen contamination, the entire melting sequence employed in this work was re-examined and compared to earlier practice in which satisfactory purity levels were obtained. A large number of chromium alloys have been induction melted and cast in these laboratories, using similar techniques, as heats ranging in size from 10 to 100 pounds. Interstitial impurity levels in these earlier alloys were well below the limit of 300 ppm total which was specified for the present program. For example, the average oxygen and nitrogen contents of 15 heats of C-207 and directly related compositions were respectively 83 and 54 ppm.

In the present series of alloys the gas contents of the starting materials, ultimate vacuua and leak rates in the melting chamber, and purity of the inert gas introduced during melting were each equal or superior to those in prior work. Crucibles and mold liners were also of the same type employed successfully in the earlier heats. Although these factors did not appear to be involved in the drastic contamination experienced in melting the Phase A alloys, they were not ignored in the sequence of revised melts which were made to identify and correct the source(s) of oxygen pick-up.

Duplicate re-analysis of the gas contents of the present lots of chromium and yttrium, which are the only two elements common to each of the contaminated heats, gave the following results:

Material	Gas Content (ppm)		
	O	N	H
Chromium Flake	49	86	1
Yttrium Sponge	730	10	25

Since the yttrium and other minor alloying elements shown previously in Table 4 were added in concentrations of less than 1 weight percent, the oxygen input from these sources amounts to only a few parts per million and cannot account for the observed contamination. Sampling of the purified argon showed a maximum oxygen content of about 5 ppm. In the furnace chamber

with a volume of 95 cubic feet, the impurities in the argon could thus add less than 15 ppm oxygen to the 4-pound alloy charges.

A number of other factors connected with melting and casting practice were considered as potential sources of oxygen contamination. These are listed below:

1. The arc hot-topping of the ingots immediately after casting.

2. Intermediate-temperature bake-out of the crucible and briquetted charge at 1300 $\pm$ 100°F under a vacuum of 10^{-4} to 10^{-3} torr.

3. Excessive superheat during the stirring cycle after adding reactive solutes.

4. Contamination from the inert gas lines, which were blanked off during leak rate determinations.

5. Increased reaction of the melt with the Y_2O_3-stabilized ZrO_2 crucible due to the larger surface area-to-volume ratio in the smaller heats, or to an inherent instability in the particular crucibles employed.

6. Reaction with the CaO-stabilized mold liner, which might be accelerated by arc hot-topping.

7. Insufficient yttrium in the charge for complete deoxidation.

8. An undetected leak, or other source of oxygen, in the furnace chamber.

A series of melts was designed to separate the effects of each of the foregoing factors on the oxygen contents of the resultant ingots. Only carbon-free alloys were used in the sequence of heats to be described below, since those alloys in the contaminated series which contained carbon additions were partially deoxidized. In the first group of revised heats, alloys which contained 0.3% Y in the briquetted charge were melted in the 50-pound furnace using crucibles and mold liners from the same lots employed in the contaminated series. The first four factors in the list above -- arc hot-topping, vacuum bake-out, superheat, and the introduction of argon -- were varied in this group. As in the contaminated alloys, samples for vacuum fusion analysis were taken from center locations at depths of 3/8 $\pm$ 1/8" from the surfaces. Specific variations in melting practice and gaseous impurity contents of the ingots are shown in Table 7.

It is clear from these data that the major portion of the oxygen contamination was caused by the intermediate-temperature (1200 - 1400°F) bake-out of the crucible and briquetted charge which had been employed in all of the contaminated series. Elimination of this step resulted in a

four-to five-fold decrease in the oxygen content. Neither the degree of superheat nor the introduction of argon appeared to influence the final oxygen level. Some indication of improvement was noted in the heat in which both the bake-out cycle and the arc hot-topping practice were dropped, but the combined interstitial contents in each of these heats were still 50 to 100% above acceptable limits.

Results to this point indicated that the remaining oxygen contamination was due to interaction with the crucibles and molds or with the furnace environment. In either case, the degree of contamination would be expected to be considerably greater in the 4-pound heats used here than in the larger heats of alloys melted in previous programs, most of which were prepared from charges of 12 to 15 pounds. The larger surface area-to-volume ratios in the smaller-diameter crucibles and mold liners used here would magnify the effects of any reaction with the ZrO_2, and the lower volume of molten metal exposed to the furnace atmosphere of a given impurity level would also result in a greater impurity concentration in the ingot. On the other hand, oxygen pick-up from either one or both of these possible sources might be reduced to acceptable levels by increasing the yttrium content in the initial charge to promote further deoxidation by slag formation. In order to separate these factors, a second group of alloys were melted and cast in the 50-pound furnace used in all Phase A work to this point and in a smaller lab furnace (NRC Model 2551) with a maximum capacity of 15 pounds and a chamber volume of 10 cubic feet. No intermediate-temperature bake-out was used and the ingots were not arc hot-topped. Yttrium contents in the briquetted charges were varied from 0.3 to 0.5%, and heats were cast into copper molds with and without the CaO-stabilized Y_2O_3 mold liners. In addition to vacuum fusion analysis for gas contents, the approximate yttrium and zirconium levels of each heat were determined by comparing in x-ray emission the respective intensities of K_α lines with those from similar chromium alloys of known yttrium and zirconium contents. Since none of the alloys contained any intentional zirconium addition, its concentration in the ingot is indicative of the degree of interaction with ZrO_2 crucibles and/or liners. Average results from cast samples taken at depths of $3/8 \pm 1/8"$ from top and bottom surfaces of ingots in this series are presented in Table 8. With the one exception noted, individual analyses varied from the averages by no more than $\pm$ 20%.

Although elimination of the arc hot-topping step and increasing the yttrium content of the charges resulted in a further reduction in the oxygen level of heats melted in the larger furnace, the results are still unsatisfactory. Some interaction with the stabilized ZrO_2 crucibles has occurred in each melting facility, but the important factor appears to be the furnace environment itself. All of the alloys melted in the 15-pound furnace, which has a chamber volume nearly 10 times smaller than that of the 50-pound furnace, have combined interstitial impurity contents well below the limit of 300 ppm. This smaller furnace is being used exclusively in replacing the Phase A alloys which were contaminated in the initial series of melts.

Each of the 4-pound heats cast directly into copper molds with no ceramic liners contained solidification cracks. Those cast into ZrO_2 mold liners and allowed to freeze without external hot-topping were free of these cracks, but had shrinkage cavities which extended 2 inches or more below the surfaces. In order to produce sound ingots of sufficient size for this program, it was therefore necessary to increase the charge weight to 7 pounds, extend the depth of the mold accordingly, and discard the portion of the ingot which contains the pipe. Briquetted charges containing 0.4% Y are being melted under conditions described previously, except,of course, that neither intermediate-temperature bake-out treatments nor arc hot-topping techniques are employed. The heats are cast through ZrO_2 tundishes into copper molds provided with ZrO_2 liners, the upper 3" of which is of 1" wall thickness to delay freezing in the hot top. At this writing, gas analyses of an additional 11 alloys prepared in this manner are available. Combined gaseous impurity levels are in the range 81 to 153 ppm and the individual concentrations of oxygen and nitrogen are below 100 ppm in each case.

Microstructural characteristics which are representative of the three general levels of purity produced in similar alloys by variations in the melting practice are illustrated in Figure 4. The grossly contaminated alloys in the initial series all contain numerous, rather massive oxide particles such as those shown for the CI-6 composition in Figure 4A. Elimination of the intermediate-temperature bake-out cycle reduced the oxygen content to about 500 $\pm$ 100 ppm, but this concentration is still considerably above the solubility limit as shown by the example in Figure 4B. Structures of the low-oxygen alloys are dependent on the residual yttrium content. Alloy CI-7A, with a retained yttrium level of approximately .10%, is free of oxide particles and shows only isolated evidence of an intergranular phase. The CI-5B alloy, which contains nearly twice as much yttrium, is structurally similar to CI-7A in that oxide particles are virtually absent, but the grain-boundary phase is much more pronounced. Although electron microprobe traces across grain boundaries showed a significant but variable decrease in both chromium (5 to 15%) and molybdenum (2 to 5%) compared to their concentrations in the matrix, there was only very slight increase in yttrium intenstiy. Scans of the entire spectrum of wave lengths emitted from such intergranular regions were conducted on the premise that this phase could be based on some low-melting metallic impurity, but only chromium, molybdenum and yttrium were detected. It is presently hypothesized that this intergranular phase is yttrium-rich, but that it was rapidly attacked by the light etching employed in sample preparation. Experiments are being repeated both in the unetched condition and after short-time air exposure of the specimens to convert any yttrium in this phase to the oxide and thereby retain its distribution.

Finally, the data in Table 8 indicate that the retained yttrium contents more nearly approach the intended values with initial charge additions of 0.4%. This concentration is employed in the series of alloys which are currently being melted and processed to replace those which were contaminated by the earlier melting practice.

EXPERIMENTAL RESULTS - PHASE B

Data from a rather large number of arc-melted buttons from several alloy systems are being generated in this phase of the program. The ultimate goal is to select the most effective of the approaches surveyed here for incorporation in larger heats to be prepared in subsequent phases of the study. Discussion of this work is arranged in terms of alloy systems of generally increasing complexity, in the same order in which they were presented earlier in Table 2. All the alloys in Phase B were arc melted as 50 to 100 gram heats using tungsten electrodes, copper button molds, and a helium atmosphere gettered prior to preparation of the buttons by melting a titanium charge. Each alloy was melted a minimum of three times to promote homogeneity.

Cr-W-V Alloys

At temperatures above 2000°F, W is one of the most effective solid-solution strengthening additions which can be made to Cr. One of the reasons that it has not received more emphasis in the first series of larger heats is that the concentration of W in binary alloys is limited to about 5 $^{a}/_{o}$ by the solid-state miscibility gap in the Cr-W system below 1800°F. Prior work indicates that V has a relatively mild strengthening effect in binary alloys with Cr, but that it increases the solubility of W in ternary alloys. Since available data are too limited to establish the solvus with any degree of accuracy, a series of alloys with 5, 7.5 and 10 $^{a}/_{o}$ W has been prepared with V additions ranging from 0 to 20 $^{a}/_{o}$. The alloys were arc melted from iodide Cr crystals and drop cast as 1/2" diameter cylinders. Sections from these castings appeared to be single-phased after 2-hour annealing at 2500°F in hydrogen. They are currently being aged for prolonged periods at 1650° and 1800°F, the range in which W-rich solid solution is rejected from binary alloys.

Co Additions To Cr-Re And Cr-Ru

Concentrations of about 35 $^{a}/_{o}$ Re and 20 $^{a}/_{o}$ Ru result in highly ductile Cr alloys. Such compositions can be cold worked from the as-cast condition and retain their ductility after exposure at elevated temperatures. As outlined in a preceding section, recent experiments have shown that Co additions to Cr at levels of 25 to 30 $^{a}/_{o}$ result in similar ductility improvements when the alloys are supersaturated by chill casting or by quenching from an annealing temperature above 2500°F. However, since the solubility of Co drops rapidly with decreasing temperature, these alloys are embrittled by sigma phase formation during aging in the temperature range of 1500° to 2000°F.

The approach adopted in the present series was to add Co to Cr-Re and Cr-Ru alloys in an attempt to decrease the amounts of Re or Ru required for significant ductility improvements. The alloys were prepared from iodide Cr crystals and Re, Co and Ru powders which were hydrogen treated at 2550°F for 1/2 hour to deoxidize and then arc melted. The ternary alloys were first melted as buttons and then drop cast into 1/2" diameter cylinders. Disks approximately 0.1" thick were cut from the cylinders and rolled at room temperature until excessive cracking occurred. Results of these rolling experiments are illustrated on the diagrams of the Cr-rich corners of the Cr-Re-Co and Cr-Ru-Co systems in Figures 5 and 6 respectively.

At the level of 11 a/o Re, the ductility shows a marked increase as the Co content increases. Little improvement in workability is noted at the lower Re content investigated. Similar behavior is observed in the Cr-Ru-Co system. Increasing the Co level results in a continuous improvement in cold rolling characteristics at the higher Ru content.

All the alloys shown in Figures 5 and 6 were single-phased in the as-cast condition. However, after heat treatment at 2550°F for 1 hour and then aging for 100 hours at 1650°F, precipitation of sigma phase occurred in most of the alloys. Aged structures of the more highly alloyed Cr-Re-Co compositions, those which in the cast condition exhibited the best cold workability, are shown in Figure 7 and metallographic observations from the entire series are summarized in Table 9. Based on these data, the tentative boundaries between the bcc solid solutions and the two-phase regions containing sigma are indicated on the ternary diagrams in Figures 5 and 6. Results obtained to date indicate that Co can in fact be substituted for relatively large protions of the Re and Ru required to promote cold workability in cast Cr alloys. Thermal stability is impaired by such substitution, however, particularly at the higher Co levels. In order to complete this work, a series of six alloys in the Cr-Re-Co system located near the 1650°F phase boundary is being prepared and will be evaluated in greater detail.

Cr-Y Alloys With Dilute Re, Ru and Co Additions

Aside from the improvement of ductility in concentrated solutions, Re has been shown in prior work to have a beneficial effect on air oxidation behavior of much more dilute Cr alloys containing Y. Since Ru and Co are analogous to Re in other respects, the oxidation-nitridation resistance of a series of Cr-Y alloys with relatively small additions of these three elements was evaluated. The alloys were prepared from hydrogen-reduced Cr flake and purified Re, Ru, and Co. The Cr was alloyed first with the Re, Ru, or Co to insure homogeneity. These buttons were crushed to provide a master alloy to which the Y was added. The alloys were first melted as buttons and drop cast into 1/2" diameter cylinders. Disks approximately 0.1" thick were cut, ground through 600 grit paper, cleaned, and exposed to air at 1500°F, 100 hours, 2100°F, 100 hours, and 2400°F for 24 hours. Results are compiled in Table 10. In general, the combination of Y and Re

results in improved oxidation-nitridation behavior. The Cr-Re-Y alloys exhibited better oxide adherence and less nitridation than similar compositions with either Ru or Co.

Photomicrographs of the representative specimens are presented in Figures 8 and 9. In none of the alloys was evidence of nitridation noted after 100 hours at 1500°F. Structures in each instance were similar to the as-cast structure. Alloys with 0.5 a/o Y contain second phase particles which are fairly uniformly distributed in an intergranular and interdendritic array. This distribution, as discussed in conjunction with the induction-melted heats in Phase A, suggests that the particles are Y-rich. The alloys with 0.1 a/o Y also contain a second phase or phases but in greatly reduced quantity.

In the Cr-4Re-0.1Y alloy, precipitation of nitride needles occurred during oxidation at 2100° and 2400°F as shown in Figures 8A and 8B. The nitridation resistance appeared to be better than that of a Cr-4Mo-.1Y alloy which will be discussed later. Nitridation resistance, particularly at 2400°F, was improved as the Y content was increased to 0.5% as shown in Figures 8C and 8D. Some agglomeration of the dispersed phase occurred at the higher temperature. Increasing the Re to 8 a/o resulted in a further improvement in nitridation resistance as indicated in Figures 9A and 9B. Again agglomeration of the second phase occurred at the higher test temperature, along with evidence of incipient melting.

The alloys with Ru and Co additions were much less resistant to air oxidation than the Re-containing alloys. Extensive nitridation occurred at 2400°F as shown in Figures 9C and 9D.

These results indicate that Re is beneficial with regard to nitridation resistance but that Ru and Co, at the 4 a/o level, are detrimental. Should any of the ternary Cr-Re-Co alloys exhibit a better balance of cold workability and thermal stability in the compositions being prepared in regions near the two-phase boundary, the air oxidation behavior of such alloys will be established before making a decision to melt larger heats.

Cr-Y Alloys With Group IV A and V A Carbides

In order to provide the best possible combination of strength, ductility and resistance to embrittlement during air oxidation in the design of dispersion-strengthened alloys in succeeding phases of the work, a critical survey of the interactions between carbide-forming elements and nitridation-inhibiting additions is being made in Phase B. Results from the first portion of that survey are presented in this section. Each of the Group IV A and Group V A metals were added at levels of 0.5 and 1.0 atomic percent to base compositions of Cr, Cr-Y, and Cr-Y-C. The alloys were arc melted as 60-gram buttons, sheathed in mild steel and drop-forged at 2200°F to a 60%

reduction in thickness. The alloys with reactive metal additions of 1.0 atomic percent were rolled to .070 ± .010" strip at 2100° - 1900°F, using initial reductions of 20% per pass at the higher temperature and finishing with 10% reductions at 1900°F.

Air oxidation tests were conducted at 2100°F on wrought samples of the entire series. Effects of oxidation on the lower-temperature mechanical properties of representative alloys with reactive metal additions of 1.0 atomic percent were compared by bend tests on sheet specimens. The as-rolled strip was cut into coupons, ground to remove surface defects and any interaction with the sheating material, annealed for one hour at 2000°F in vacuum of 10^{-5} torr, and electropolished at a current density of about 1 amp/in^2 in a 10% perchloric -90% acetic acid electrolyte maintained at or below 50°F. One sample was tested in this condition. Additional specimens were oxidized in static air for 100 hours at 2100°F and, if sufficient material was available, at 1500°F. The latter oxidation temperature was included since prior work has shown significant embrittlement of similar Cr alloys during air exposure at 1200° - 1600°F, even in compositions which have high resistance to nitridation at 2000°F and above. Bend tests were made in an Instron machine at a ram speed of .05 ipm using a die radius of 4T where T is the sheet thickness. Ductile-brittle transition temperatures (DBTT) were approximated by a single-specimen testing technique in which the sample was bent through an angle of 15° at the intital test temperature, then through additional bends of 15° at successively lower temperatures until fracture occurred. In the rolled and annealed condition, initial tests were made at 400°F and the temperature was lowered in decrements of 50° - 100°F. Tests of oxidized specimens were started at 800°F and decrements of 100° - 200°F were employed. The DBTT is here defined as the lowest temperature at which the specimen underwent a 15° bend without fracture. Values of the load at departure from linearity on automatically recorded load-time curves at the initial test temperature were used in the determination of flow stresses, which of course should not be considered as accurate measures of the proportional limit.

Results of 2100°F oxidation tests of the entire series are shown in Table 11 and mechanical properties of representative alloys are summarized in Table 12. Rather marked differences in both oxidation and mechanical behavior are observed between those alloys containing additions of Group IV A metals (Ti, Zr, and Hf) and those with solutes from Group V A (V, Cb and Ta). Each of the elements in binary alloys with Cr at the level of 0.5 atomic percent results in an increase in the oxidation rate over that of the unalloyed metal at 2100°F. However, small additions of Y to the alloys with Group IV A solutes are very effective in reducing oxidation, whereas Y is relatively ineffective when added to binary alloys with V, Cb, or Ta. The same trends are observed in similar alloys with C. Even without Y, the alloys with ZrC and HfC exhibit weight-gain values considerably below those with the other four carbides. Additions of Y in general result in lower oxidation rates in those compositions which contain carbides based on the Group IV A metals. The alloys with VC are an exception to this

trend, in that quite low weight gain values are obtained in the presence of Y, particularly at the higher nominal concentration of 0.2 atomic percent. It should also be noted that the alloys with carbides based on Group IV A metals have somewhat lower rates of oxidation at the higher metal-to-carbon ratio, while the reverse appears to be the case for those with carbides of V, Cb and Ta.

Differences in low-temperature mechanical properties and in the effects of oxidation on ductility, which are summarized in Table 12, are also pronounced. Alloys with TiC, CbC and TaC have considerably higher strengths and somewhat higher DBTT values in the rolled and annealed condition. Air exposure at 1500° and 2100°F results in a sharp decrease in ductility, particularly in the case of the CbC and TaC alloys. The compositions which contain ZrC, HfC and VC are ductile near or below room temperature and the former two types exhibit much better retention of ductility after air oxidation. DBTT values of 200° to 400°F were measured in oxidized Cr-Y-C alloys with Zr or Hf, compared to greater than 800°F in similar compositions containing Cb or Ta.

Some of the factors which are involved in the differences in both mechanical and oxidation behavior can be illustrated by the photomicrographs in Figure 10. Carbides in the alloys with Zr, which are typical in this respect of those with Hf, are rather coarse and widely spaced. This morphology results from the restricted solubility of Zr and Hf in Cr. Carbides are formed as grain boundary networks during solidification. These intergranular carbides are fragmented during processing, but are not appreciably altered by heat treatment. Such a coarse distribution does not have a large effect on either strength or ductility in the rolled and annealed condition. The particles are also too widely spaced to influence reaction during air exposure. Note in Figure 10A that only those few particles which intersect the surface appear to be affected by oxidation at 1500°F. At the higher oxidation temperature, the large carbides act as sinks for the gaseous contaminants as shown in Figure 10B, and no surface or intergranular nitrides are formed.

Carbides in the alloys with Cb or Ta additions are present in the form of fine, uniform dispersions which are much more effective in increasing the strength and result in somewhat lower ductility in the rolled and heat treated condition. The further losses in ductility during intermediate-temperature in exposure are probably related to additional precipitation of interstitials, both from the matrix and from inward diffusion of oxygen or nitrogen, and a resultant interaction with the dislocation array. Although essentially no subsurface hardening was observed at 1500°F in the Cr-Y alloys with ZrC or HfC additions, those containing Cb or Ta were hardened by 25-50 DPH to depths of 4 to 6 mils. Oxidation at the higher temperature results in accelerated reaction of alloys with CbC or TaC dispersions. The particles are closely enough spaced that they present a semi-continuous oxidation front. They are rapidly saturated by the gaseous contaminants, and both surface and intergranular nitrides are formed as

illustrated in Figure 10D. Even in the absence of C, additions of Cb and Ta appear to at least partially negate the beneficial effects of Y on oxidation behavior, as indicated by the weight gain data in Table 11. As noted previously, this is not the case with solutes from Group IV A.

Alloys with VC appear to have the poor features of each type discussed above, without the attractive properties of either. A relatively fine dispersion is formed during cooling from high temperatures, but the thermal stability is quite low. Rapid agglomeration occurs upon heat treatment at temperatures as low as 2000°F. Although the ductility of the alloys with V is good, their strengths are not greatly different than those of a Cr-Y binary and they are severely embrittled by oxidation at 2100°F. Structures of the alloys with TiC are similar to those with CbC in that a fine dispersion is formed. Embrittlement due to oxidation is not as great, however, since Ti additions, unlike those of Group V A solutes, do not interfere with the effects of Y.

Based on this survey, the choice of a combination of Zr and Ti as the "standard" carbide-stabilizing addition in the initial phases of Task I appears to be justified. Superior strengths, however, can be attained with Cb-rich or Ta-rich carbides. It is possible that embrittlement of such alloys can be minimized by the identification of an element which provides more effective resistance to oxidation and nitridation than does Y. Results of the initial study of this factor are presented in the following section.

Alternate Nitridation-Inhibitors In Cr-4Mo Alloys

In this group of alloys, several reactive metals were evaluated with respect to their effect on the nitridation resistance of the standard Cr-4Mo matrix. Since they closely resemble Y, emphasis was placed on the lighter rare earths from the lanthanide and actinide series, including mischmetal which is a naturally occurring mixture of the lighter elements in the former series. Additons of Be from Group II A were also investigated. The alloys were prepared from hydrogen-reduced Cr flake. A master alloy of Cr-4Mo was first arc melted as 100-gram buttons which were crushed and blended. The reactive additions were then added at levels of 0.1 and 0.5 atomic percent by arc melting and drop casting into 1/2" diameter cylinders.

Oxidation tests were conducted in static air at 1500°, 2100° and 2400°F. The weight change data are recorded in Table 13. Comparison of the total and net weight change values gives a good indication of the oxide adherence. In addition to considerable spalling at 2400°F in most of the alloys with reactive solute concentrations of 0.1 atomic percent, there was also evidence of volatile reaction products, particularly is the Cr-Mo and Cr-Mo-Be alloys. This behavior probably reflects formation of the volatile oxide CrO_3, as has been noted in a number of previous investigations at temperatures as low as 2150°F.

A summary of metallographic observations and hardness measurements of the oxidized specimens is presented in Table 14. No nitriding was detected after 1500°F exposure. In general, the alloys which exhibit a high degree of oxide adherence are also quite resistant to nitridation at the higher temperatures. Additions of La and Pr are more effective than Y in improving the air oxidation resistance of the Cr-4Mo base, and additions of mischmetal are at least equivalent. Photomicrographs of representative specimens are shown in Figures 11 and 12. The Cr-4Mo alloy is extensively nitrided at both 2100° and 2400°F. Addition of Y at the level of 0.1 atomic percent prevents the formation of continuous surface nitride layers, but as shown in 11C and 11D, some intergranular nitridation and precipitation of nitride needles within the grains is still observed at each temperature. Increasing the Y content to 0.5 atomic percent results in a further increase in nitridation resistance. Intergranular nitridation is virtually eliminated at 2400°F but, as shown in Figure 12A, there are some nitride needles evident and incipient melting occurs at this temperature. The same melting behavior was also noted at this concentration of Y in Cr alloys with Re, Ru, and Co as illustrated earlier in Figure 8. The eutectic temperature of such Cr-rich alloys with Y is thus below 2400°F and the terminal solubility of Y at the eutectic is well below 0.5 atomic percent. In fact, the cast structure of the induction-melted Cr-W-Y alloy in Figure 4D suggests that the eutectic solubility may be below 0.2 atomic percent.

Structures of the alloys with the three most effective rare-earth solutes are shown in Figures 12B through 12D. The alloy with the higher concentration of mischmetal, which consists of 50% Ce plus approximately 25% La, 15% Nd and 10% Pr by weight, exhibits very slight intergranular attack. Additions of 0.5 atomic percent lanthanum or praseodymium to the Cr-4Mo alloy completely prevent nitridation in 24-hour air exposure at 2400°F. Some minor agglomeration of the second phase, which is presumed to be rich in the rare earth metal, is observed in the alloys with Pr and mischmetal additions, but the Cr-Mo-La alloy is virtually unchanged from the as-cast condition. No evidence of incipient melting at 2400°F was detected in any of the three alloys.

Since Y additions appear to be limited to about 0.2 atomic percent or below by eutectic melting, more complex carbide-containing alloys are being prepared with La and Pr replacing Y as the nitridation-inhibitor.

CONCLUSIONS

1. Revisions in induction melting and casting techniques have consistently yielded ingots with total oxygen plus nitrogen contents below 150 ppm. The major factor in the oxygen contamination of the initial group of alloys was a bake-out treatment of the crucible and charge at 1200°-1400°F under vacuua of 10^{-4} to 10^{-3} torr.

2. Cold workability can be attained in single-phase Cr-Re-Co and Cr-Ru-Co alloys. Although intermediate-temperature aging results in sigma phase formation in many such alloys, the results have indicated promising compositional areas for further study.

3. The air oxidation resistance of Cr-Y alloys with relatively small concentrations of Re is superior to that of similar alloys with either Ru or Co.

4. Dilute Cr-Y alloys with ZrC and HfC dispersions are ductile in bending at room temperature and are more resistant to embrittlement by air oxidation than alloys containing carbides of V, Ti, Cb or Ta. Carbides formed by the latter three elements, however, are much more finely dispersed and warrant further consideration.

5. Additions of 0.5 atomic percent La or Pr are much more effective than an equivalent level of Y in preventing nitridation of a Cr-4Mo base in air oxidation at 2400°F, and do not appear to result in incipient melting as does Y at this concentration.

Materials Development Laboratory
General Electric Company
Evendale, Ohio, October 25, 1965

TABLE 1

TENSILE PROPERTIES OF WROUGHT CHROMIUM ALLOYS

Composition (Atomic %)						2000°F Tensile Properties			DBTT (°F)[b]	
Ti	Zr	Hf	Y	C	Cr	UTS (ksi)	0.2% Offset (ksi)	Elong. (%)	4T Bend*	Tensile**
--	--	--	.16	--	Bal.	9.4	7.7	18.0	50	75-100
2.8	.3	--	a	2.3	"	22.4	17.7	59.0	--	> 600
2.6	.2	--	a	1.4	"	18.4	13.8	48.0	--	> 400
1.3	.1	--	.04	.8	"	19.9	15.8	28.8	350	--
.2	.4	--	a	.4	"	24.5	19.1	24.0	-50	-30
.2	.1	.3	a	.4	"	24.7	20.3	27.0	< 50	--
.2	.2	.2	a	.5	"	26.9	24.7	24.6	100	150

a) Yttrium added to each alloy; less than .01% retained.

b) Ductile-brittle transition temperature, based on:

* 105° bends in .060" strip at ram speed of .05 ipm. Annealed 2000°F.

** 5% elongation in .160" diameter bars at strain rate of .01 per minute. Stress-relieved at 1800°F.

TABLE 2 COMPOSITIONS OF CHROMIUM ALLOYS

PHASE A - TASK I

Designation[a]	Composition (Atomic %)
CI-1	Cr-.1Y
CI-2	Cr-.2Y
CI-3	Cr-.1Y-.05Hf-.03Th
CI-4	Cr-4Mo-.1Y
CI-5	Cr-6Mo-.1Y
CI-6	Cr-8Mo-.1Y
CI-7	Cr-4W-.1Y
CI-8	Cr-6W-.1Y
CI-9	Cr-4Mo-2W-.1Y
CI-10	Cr-6Mo-2W-.1Y
CI-11	Cr-4V-.1Y
CI-12	Cr-10V-.1Y
CI-13	Cr-20V-.1Y
CI-14	Cr-10V-4Mo-.1Y
CI-15	Cr-10V-4W-.1Y
CI-16	Cr-4Re-.1Y
CI-17	Cr-4Co-.1Y
CI-18	Cr-8Co-.1Y
CI-19	Cr-.05Y-.4Zr-.2Ti-.4C
CI-20	Cr-.1Y-.4Zr-.2Ti-.4C
CI-21	Cr-.05Y-.3Hf-.3Zr-.4C
CI-22	Cr-.05Y-.4Zr-.2Ti-.4B
CI-23	Cr-.05Y-.3Hf-.3Zr-.4B
CI-24	Cr-.05Y-.4Ta-.2Zr-.4B
CI-25	Cr-4Mo-.05Y-.4Zr-.2Ti
CI-26	Cr-4Mo-.1Y-.4Zr-.2Ti
CI-27	Cr-4Mo-.1Y-.3Hf-.3Zr
CI-28	Cr-4Mo-.1Y-.05Hf-.03Th
CI-29	Cr-4Mo-.05Y-.4Zr-.2Ti-.4C
CI-30	Cr-4Mo-.1Y-.4Zr-.2Ti-.4C
CI-31	Cr-4Mo-.05Y-.5Zr-.25Ti-.4C
CI-32	Cr-4Mo-.05Y-.3Zr-.15Ti-.4C
CI-33	Cr-4Mo-.05Y-.6Ti-.4C
CI-34	Cr-4Mo-.05Y-.6Zr-.4C
CI-35	Cr-4Mo-.05Y-.6Hf-.4C
CI-36	Cr-4Mo-.05Y-.6Cb-.4C
CI-37	Cr-4Mo-.05Y-.3Hf-.3Zr-.4C
CI-38	Cr-4Mo-.05Y-.6Zr-.3Ti-.6C
CI-39	Cr-6Mo-.05Y-.2Zr-.1Ti-.2C
CA-1	Unalloyed Cr
CA-2	Cr-35Re

[a]CI - Cast, Induction Melted
CA - Cast, Arc Melted

TABLE 3 SUMMARY OF SMALL HEATS, PHASE B - TASK I

	System	Reason	Approximate Number
(1)	Cr-W-V	Increase solubility of W	10
(2)	Cr-Re(Ru)-Co	Inexpensive Re analog	9 to 12
(3)	Cr-Y-(Re,Ru,Co)	Oxidation resistance at low concentration	6 to 9
(4)	Cr-(Y)-(C)-Group IV & V Metals	Reactive solute interactions	30 to 40
(5)	Cr-Y-Si-(Cb)	Intermetallic dispersions	5 to 10
(6)	"Standard" matrix + (La,Ce,Be, etc.)	Alternate nitridation inhibitors	10 to 15
(7)	"Standard" ZTC + (6)	Carbide interaction with best from (6)	5 to 10
(8)	"Standard" matrix + best (4) + best (7)	Optimum minor solutes in S.S. matrix	5 to 10

TABLE 4

ANALYSES OF RAW MATERIALS USED IN ALLOYS OF PHASE A

Element	Purity	Form	Impurities (ppm)									
			O	N	H	C	Fe	Ni	Al	Si	S	Other
Chromium	99.94%	H_2-reduced flake	40	100	3	80	20	10	5	80	70	-
Chromium	99.997%	Iodide crystal	7	1	.5	9	13	1	.3	10	-	2Ca
Yttrium	99.9%	Sponge	890	8	-	-	20	-	5	50	-	10Ca
Molybdenum	99.9%	Pellets	105	12	-	-	160	61	25	55	-	435W
Tungsten	99.95%	Granules	80	10	-	20	10	20	10	10	-	160Mo
Vanadium	99.9%	Granules	700	50	10	200	-	-	-	-	-	-
Rhenium[a]	99.7%	Powder	1900	150	-	40	Less than 100 ppm total metallics					
Cobalt	99.5%	Shot	140	-	5	100	1100	1700	340	60	60	90Cu
Zirconium[b]	99.8%	Crystal bar	250	20	90	150	20	15	40	50	-	0.9%Hf
Titanium	99.5%	Sheet	1050	130	30	290	800	-	300	-	-	500Sn
Hafnium[b]	99.9%	Crystal bar	160	15	-	70	200	-	15	25	-	1.6%Zr
Columbium	99.8%	EB melted	250	80	-	100	< 100	-	-	<100	-	1000Ta

[a]Oxygen content reduced to less than 100 ppm by H_2 treatment at 2550°F.

[b]Purity refers to combined Zr and Hf contents.

TABLE 5

EXTRUSION DATA, FIRST GROUP OF PHASE A ALLOYS

Alloy	Extrusion No.	Temp (°F)	Glass Lubricant[a]	Extrusion Force (Tons) Upset	Extrusion Force (Tons) Average	Speed in/sec
CI-1	361	2000	7052	260	240	2
CI-2	344	2000	7052	240	240	2
CI-3	345	2000	7052	225	225	-
CI-4	362	2700	7740	280	280	1
CI-5	354	2700	7740	225	225	3
CI-6	356	2750	7740	240	225	2
CI-7	357	2750	7740	210	190	3
CI-8	358	2750	7740	240	225	3
CI-9	369	2750	7740	240	220	2.5
CI-10	370	2750	7740	240	220	5
CI-11	364	2500	7052	180	175	3.5
CI-12	365	2500	7052	210	190	3.5
CI-19	346	2200	7052	200	170	2.5
CI-20	347	2200	7052	210	200	3
CI-21	348	2200	7052	200	200	2.5
CI-22	363	2200	7052	180	180	3
CI-23	359	2200	7052	240	240	2
CI-25	360	2700	7740	240	225	5

[a]Corning Designation

TABLE 6

IMPURITY ANALYSIS OF REPRESENTATIVE PHASE A ALLOYS

Alloy	Nominal Composition (At.%)	Interstitial Content (ppm)[a]			
		O	N	C	H
CI-1	Cr-.1Y	3090	78	90	3
CI-2	Cr-.2Y	2420	98	45	12
CI-4	Cr-4Mo-.1Y	2210	59	70	11
CI-6	Cr-8Mo-.1Y	2020	50	75	6
CI-7	Cr-4W-.1Y	2160	61	35	6
CI-9	Cr-4Mo-2W-.1Y	1630	71	30	4
CI-11	Cr-4V-.1Y	2490	76	70	5
CI-19	Cr-.05Y-.4Zr-.2Ti-.4C	910	56	750	7
CI-20	Cr-.1Y-.4Zr-.2Ti-.4C	710	68	750	4
CI-21	Cr-.05Y-.3Hf-.3Zr-.4C	820	56	600	5
CI-25	Cr-4Mo-.05Y-.4Zr-.2Ti	1830	64	40	4

[a]Residual yttrium level of each alloy less than .06% by weight (the limit of detection by quantitative x-ray emission)

TABLE 7

REVISED HEATS MELTED IN 50-POUND FURNACE

Alloy	Melting Variables	Gas Content (ppm)		
		O	N	H
CI-25A	1300°F bakeout, no arc hot-topping.	2230	58	7
CI-26A	Outgassed at room temperature. Arc hot-topped.	482	65	5
CI-27A	Outgassed at room temperature. Entire heating cycle under argon. Superheat reduced 50%. Arc hot-topped.	587	64	7
CI-5A	Outgassed at room temperature. Entire heating cycle under vacuum. Superheat reduced 50%. Arc hot-topped.	522	90	3
CI-8A	Outgassed at room temperature. Heating cycle under vacuum. No arc hot-topping.	390	85	6

TABLE 8

EFFECTS OF FURNACE AND CASTING VARIABLES ON CHROMIUM ALLOY PURITY

Alloy	Heat Size (Lb)	Mold	Furnace	Yttrium in Briquette (Wt %)	Gas Content (ppm)			Approx. Analysis (Wt %)[a]	
					O	N	H	Y	Zr
CI-8A	4	ZrO_2	50-Pound	0.3	390	85	6	<.06	.08
CI-6A	4	Cu	50-Pound	0.5	329	45	8	.14	.06
CI-6B	7	ZrO_2	50-Pound	0.5	170[b]	58	8	.17	.06
CI-4A	4	ZrO_2	15-Pound	0.3	37	133	7	<.06	<.04
CI-5B	4	Cu	15-Pound	0.5	34	72	6	.19	.09
CI-7A	7	ZrO_2	15-Pound	0.4	29	69	11	.10	.05
CI-9A	7	ZrO_2	15-Pound	0.4	22	76	7	.15	.07

[a]From semi-quantitative x-ray emission.

[b]Triplicate analyses yielded values of 62, 315, and 132 ppm oxygen.

TABLE 9

COMPOSITIONS AND METALLOGRAPHIC OBSERVATIONS
IN CR-RE-CO AND CR-RU-CO ALLOYS

Composition (At. %)		Metallographic Observations Aged 100 Hrs. at 1650°F	
Co	Re, Ru	Structure	Microhardness DPH, 1Kg Load
5.6	10.9 Re	Single Phase	462
11.5	11.0 Re	Slight Ppt.	591
5.2	6.7 Re	Single Phase	443
10.5	6.7 Re	Slight Ppt.	584
17.2	11.0 Re	Approx. 50% sigma	804
23.1	11.1 Re	Approx. 80% sigma	957
9.7	8.5 Ru	Approx. 10% sigma	504
14.5	8.5 Ru	Approx. 40% sigma	674
4.8	8.4 Ru	Single Phase	434
4.5	5.5 Ru	Single Phase	426
9.5	5.5 Ru	Slight Ppt.	514

TABLE 10

OXIDATION DATA FROM CR-Y ALLOYS
WITH RE, RU AND CO ADDITIONS

Nominal Composition (At. %)	Wt. Change Data (mg/cm^2)[a]				
	1500°F, 100 Hrs.	2100°F, 100 Hrs.		2400°F, 24 Hrs.	
		Total	Net	Total	Net
4Re, 0.1Y	0.84	3.63	3.59	4.3	3.8
4Re, 0.5Y	0.87	3.87	3.83	2.05	1.63
8Re, 0.1Y	1.61	6.22	6.06	11.1	9.8
8Re, 0.5Y	0.76	0.87	0.79	1.2	0.53
4Ru, 0.1Y	0.60	4.02	3.26	2.17	-14.5
4Ru, 0.5Y	1.15	4.97	4.73	6.67	1.21
4Co, 0.1Y	0.65	1.17	-3.56	0.84	-15.0
4Co, 0.5Y	1.07	5.28	4.75	8.15	2.2

[a]Net weight change denotes the total weight gain less the weight of the loose oxide.

TABLE 11

EFFECTS OF SOLUTES FROM GROUPS IV A AND V A
ON THE AIR OXIDATION OF CR-Y-C ALLOYS

Nominal Composition (At. %)	100-Hour Weight Gain (mg/cm^2) at 2100°F[a]					
	M = Ti	Zr	Hf	V	Cb	Ta
Cr-.5M	18.9	13.3	16.1	-	22.3	19.3
Cr-.5M-.1Y	2.7	1.4	2.8	12.8	12.2	14.2
Cr-.5M-.2Y	2.3	2.5	1.9	13.1	11.3	11.4
Cr-.5M-.4C	14.2	4.6	8.2	-	20.8	17.8
Cr-.5M-.4C-.1Y	4.6	3.0	5.7	3.0	18.1	12.9
Cr-.5M-.4C-.2Y	4.8	2.9	4.0	1.8	10.0	13.3
Cr-1M-.4C	11.9	3.7	6.6	10.2	33.1	-
Cr-1M-.4C-.1Y	2.5	3.0	2.3	8.4	24.5	13.9
Cr-1M-.4C-.2Y	2.3	2.2	3.4	2.3	12.5	-

[a]The 100-hour weight gains of unalloyed Cr and Cr-.1Y are 12.7 and 2.0 mg/cm^2, respectively, at 2100°F.

TABLE 12

LOW-TEMPERATURE BEND PROPERTIES OF SELECTED CARBIDE-STRENGTHENED CHROMIUM ALLOYS AND EFFECTS OF AIR OXIDATION

Nominal Composition (At. %)	Rolled + Annealed			1500°F-100 Hr.-Air		2100°F-100 Hr.-Air	
	DPH (kg/mm^2)[a]	DBTT (°F)[b]	400°F σ_D (ksi)[c]	DBTT (°F)	800°F σ_D (ksi)	DBTT (°F)	800°F σ_D (ksi)
Cr-.1Y	138	-50	18.1	< 75	11.4	100	14.2
Cr-1Ti-.4C	216	200	79.0	800	74.3	> 800	47.7
Cr-1Ti-.4C-.1Y	217	200	72.1	500	65.5	600	49.4
Cr-1Zr-.4C	161	75	48.6	400	41.7	800	37.4
Cr-1Zr-.4C-.1Y	152	0	47.1	200	58.8	300	35.7
Cr-1Zr-.4C-.2Y	156	75	55.3	400	41.0	200	27.5
Cr-1Hf-.4C-.1Y	172	150	42.4	200	59.7	400	25.8
Cr-1Hf-.4C-.2Y	160	100	50.4	-	-	200	31.5
Cr-1V-.4C	140	75	19.0	-	-	> 800	15.0
Cr-1V-.4C-.1Y	142	-50	17.3	200	24.7	> 800	26.1
Cr-1V-.4C-.2Y	149	100	28.5	-	-	Broke in handling	
Cr-1Cb-.4C	215	300	74.1	> 800	69.5	Broke in handling	
Cr-1Cb-.4C-.1Y	199	200	77.2	800	80.1	> 800	68.6
Cr-1Ta-.4C-.1Y	224	300	82.9	-	-	> 800	70.5

a) Diamond pyramid hardness, 100 gram load.

b) Ductile-brittle transition temperature based on 15° deflection in 4T bend tests at a ram speed of .05 ipm.

c) σ_D denotes fiber stress at deviation from linearity on load-time curves at indicated temperatures.

TABLE 13

EFFECT OF SELECTED REACTIVE METALS ON THE AIR OXIDATION OF CR-4MO ALLOYS

Nominal Composition (At. %)	Weight Change Data (mg/cm^2)[a]				
	1500°F-100 Hrs.	2100°F-100 Hrs.		2400°F-24 Hrs.	
		Total	Net	Total	Net
4Mo	0.83	12.1	7.93	1.32	-15.6
4Mo-0.1Y	0.87	3.27	3.27	4.6	0.15
4Mo-0.5Y	1.52	2.80	2.76	6.2	5.7
4Mo-0.1Ce	0.95	2.38	2.26	6.55	- 0.8
4Mo-0.5Ce	0.84	1.63	1.63	6.4	5.0
4Mo-0.1La	0.76	-0.38	-0.38	1.86	- 0.95
4Mo-0.5La	0.69	0.8	0.72	2.2	1.71
4Mo-0.1Th	1.38	8.2	7.3	14.0	5.1
4Mo-0.5Th	1.72	5.0	5.0	10.25	2.7
4Mo-0.1Pr	0.87	1.03	1.03	5.3	1.63
4Mo-0.5Pr	0.72	0.95	0.76	3.4	- 0.1
4Mo-0.1Be	0.76	8.2	7.0	1.63	-11.8
4Mo-0.5Be	0.72	5.5	3.8	- .57	- 5.75
4Mo-0.1MM[b]	0.87	2.64	2.53	5.65	2.64
4Mo-0.5MM	0.20	1.68	1.56	4.5	3.5

[a] Net weight change denotes total gain less the weight of loose oxide.

[b] Mischmetal: 50% Ce + 50% (La, Nd and Pr)

TABLE 14

METALLOGRAPHIC OBSERVATIONS OF AIR OXIDATION EFFECTS
IN ALLOYS WITH ALTERNATE NITRIDATION INHIBITORS

Nominal Composition (At. %)	1500°F-100 Hrs.[a]	2100°F-100 Hrs.		2400°F-24 Hrs.	
	DPH[b]	DPH[b]	REMARKS[c]	DPH[b]	REMARKS[c]
4Mo	280	296	GBN + layer	298	Extensive nitride
4Mo-0.1Y	282	305	GBN + needles	305	GBN
4Mo-0.5Y	271	286	Needles	285	Needles
4Mo-0.1Ce	271	298	GBN + needles	294	GBN
4Mo-0.5Ce	262	292	Needles	291	GBN
4Mo-0.1La	255	270	GBN + needles	295	GBN + needles
4Mo-0.5La	249	239	No nitride	260	No nitride
4Mo-0.1Th	-	-	GBN	-	GBN + layer
4Mo-0.5Th	-	-	GBN	-	Extensive nitride
4Mo-0.1Pr	256	275	Needles	275	GBN
4Mo-0.5Pr	277	270	No nitride	278	No nitride
4Mo-0.1Be	-	-	GBN + layer	-	Extensive GBN
4Mo-0.5Be	-	-	GBN	-	Extensive GBN
4Mo-0.1MM	265	295	GBN	278	GBN
4Mo-0.5MM	267	295	No nitride	309	Small amt. GBN

[a] No nitrides observed in any of the alloys after 1500°F air exposure.

[b] Diamond Pyramid Hardness - 100 gm load. Average matrix hardness does not include grain boundary nitrides.

[c] GBN denotes grain boundary nitride.

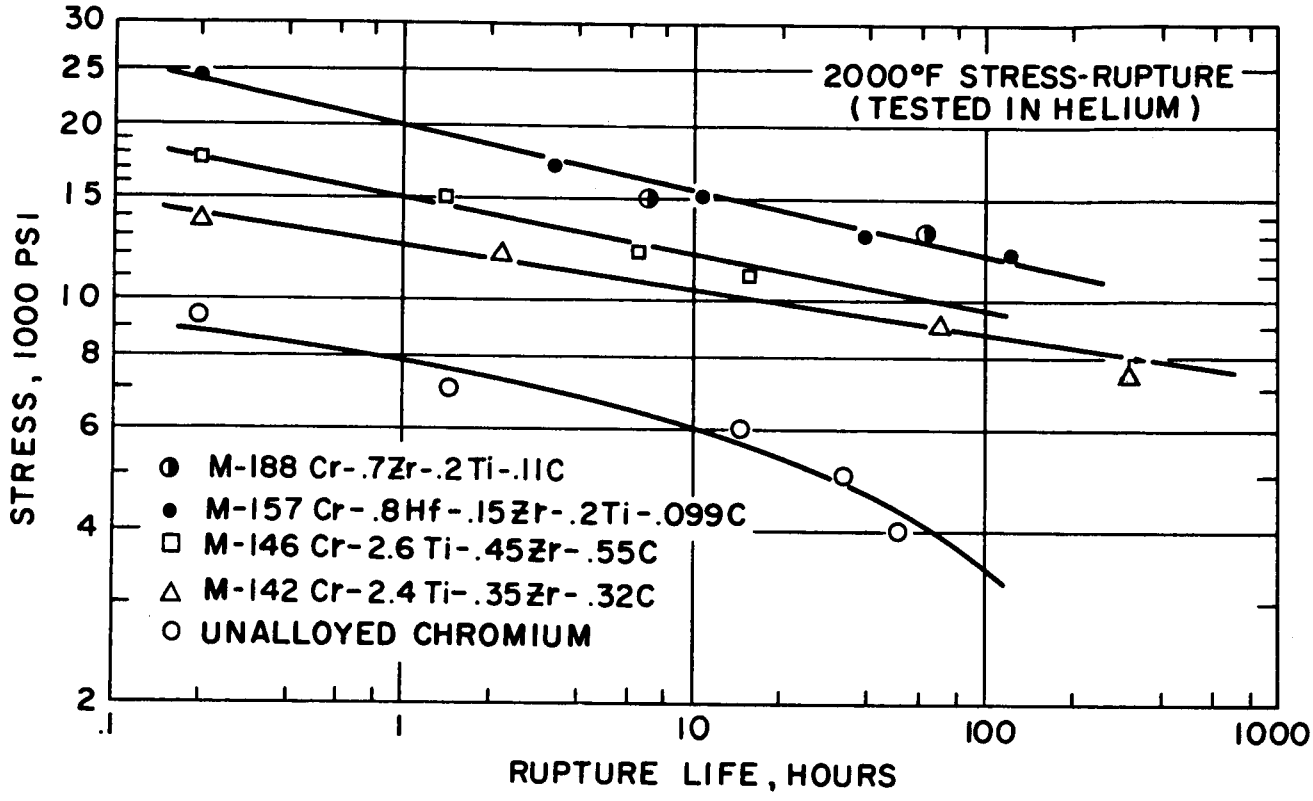

Figure 1. Stress-Rupture Properties of Wrought, Carbide-Strengthened Chromium Alloys. (Compositions in Weight Percent)

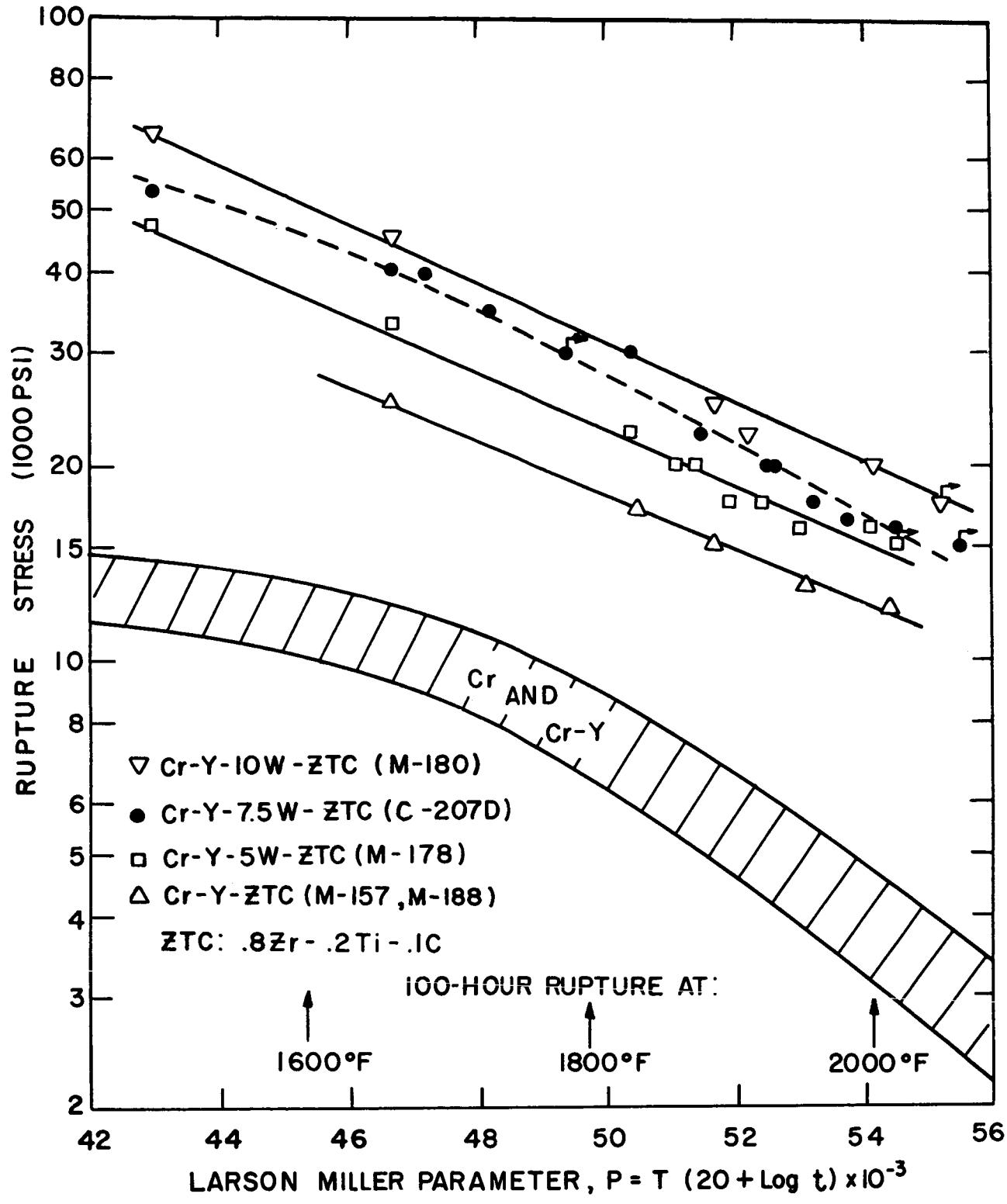

Figure 2 Stress-Rupture Properties of Wrought Chromium Alloys Tested in Helium Atmosphere. (Compositions in Weight Percent)

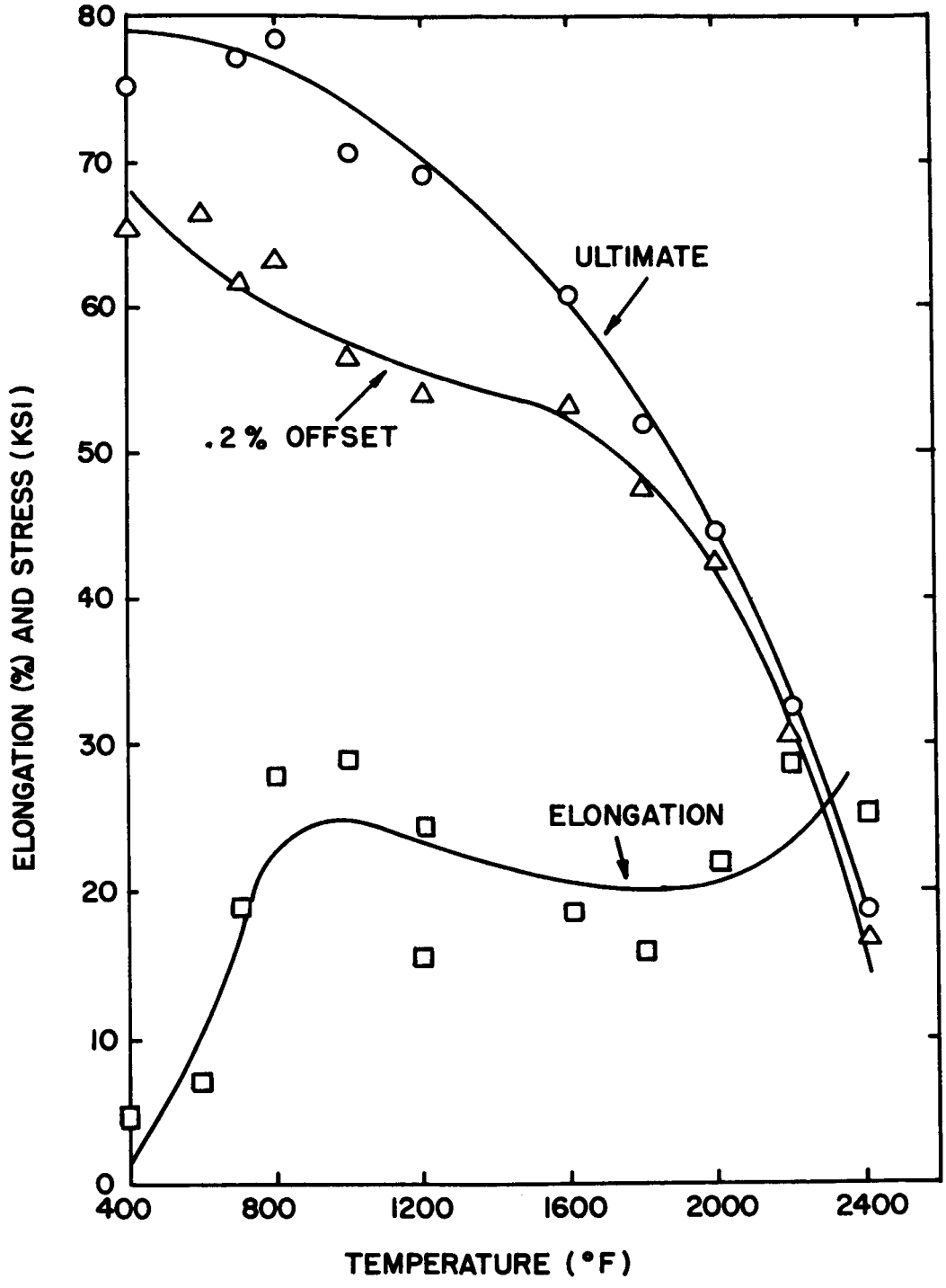

Figure 3 Tensile Properties of Chromium Alloy C-207F

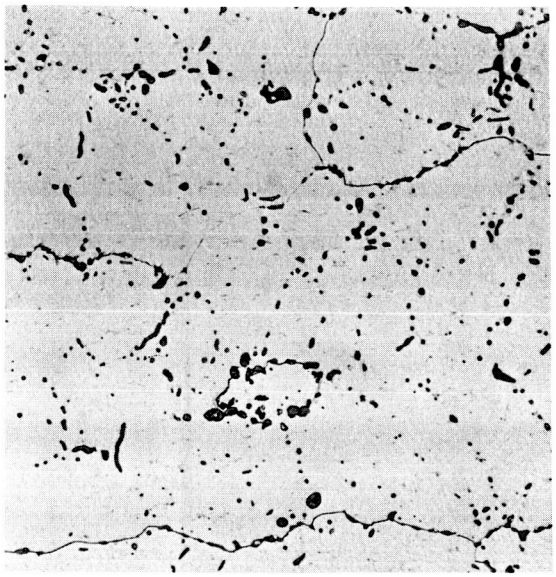

L2955 250X

A. Alloy CI-6 (.202% O_2, <.06% Y)

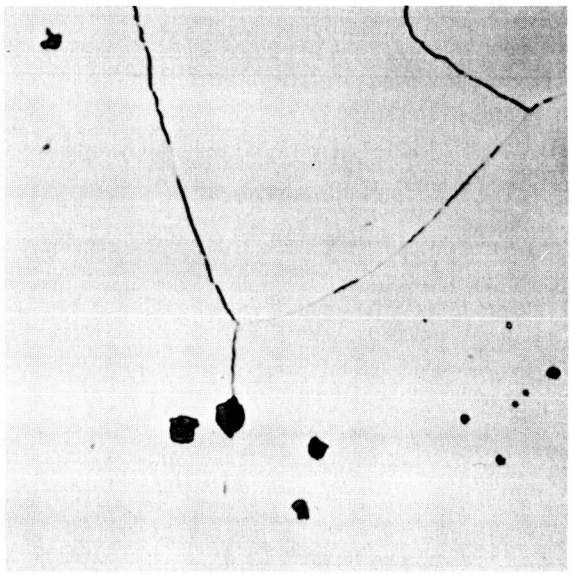

L3781 1000X

B. Alloy CI-5A (.0522% O_2, <.06% Y)

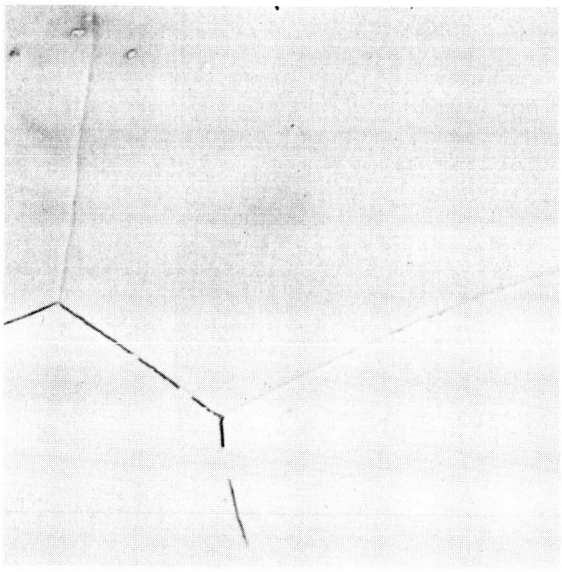

L3784 1000X

C. Alloy CI-7A (.0029% O_2, .10% Y)

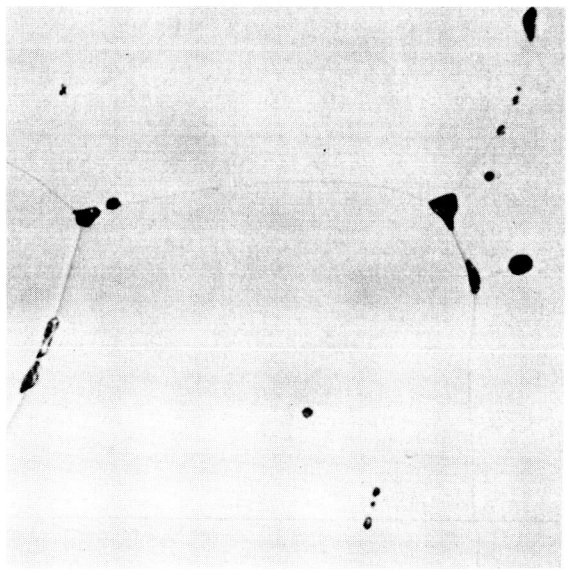

L3780 1000X

D. Alloy CI-5B (.0034% O_2, .19% Y)

Figure 4. Cast structures of induction-melted Cr alloys at indicated oxygen and yttrium levels (weight %). Etched 10% oxalic acid.

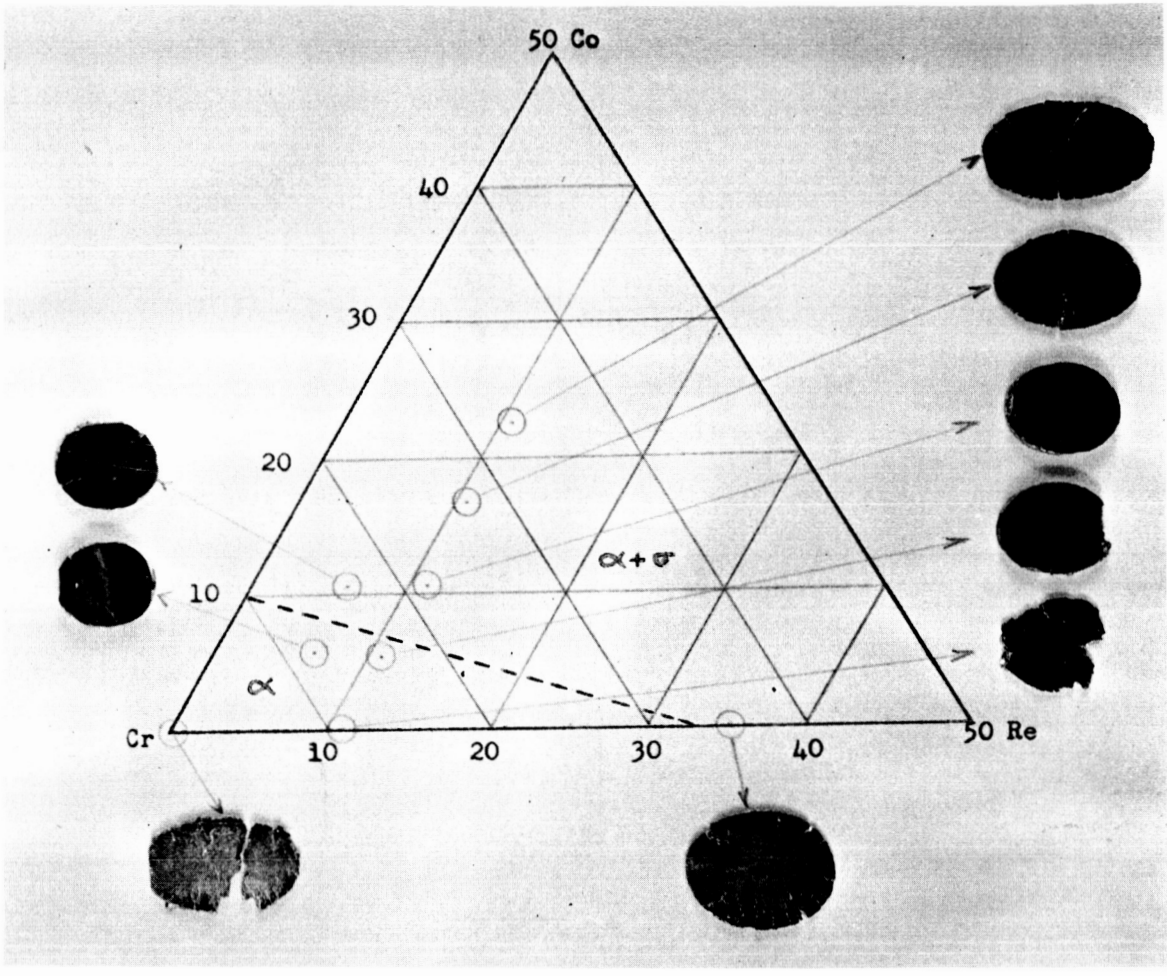

Figure 5. Cold workability of drop cast Cr-Re-Co alloys with compositions shown in atomic %. Tentative phase boundary at 1650°F.

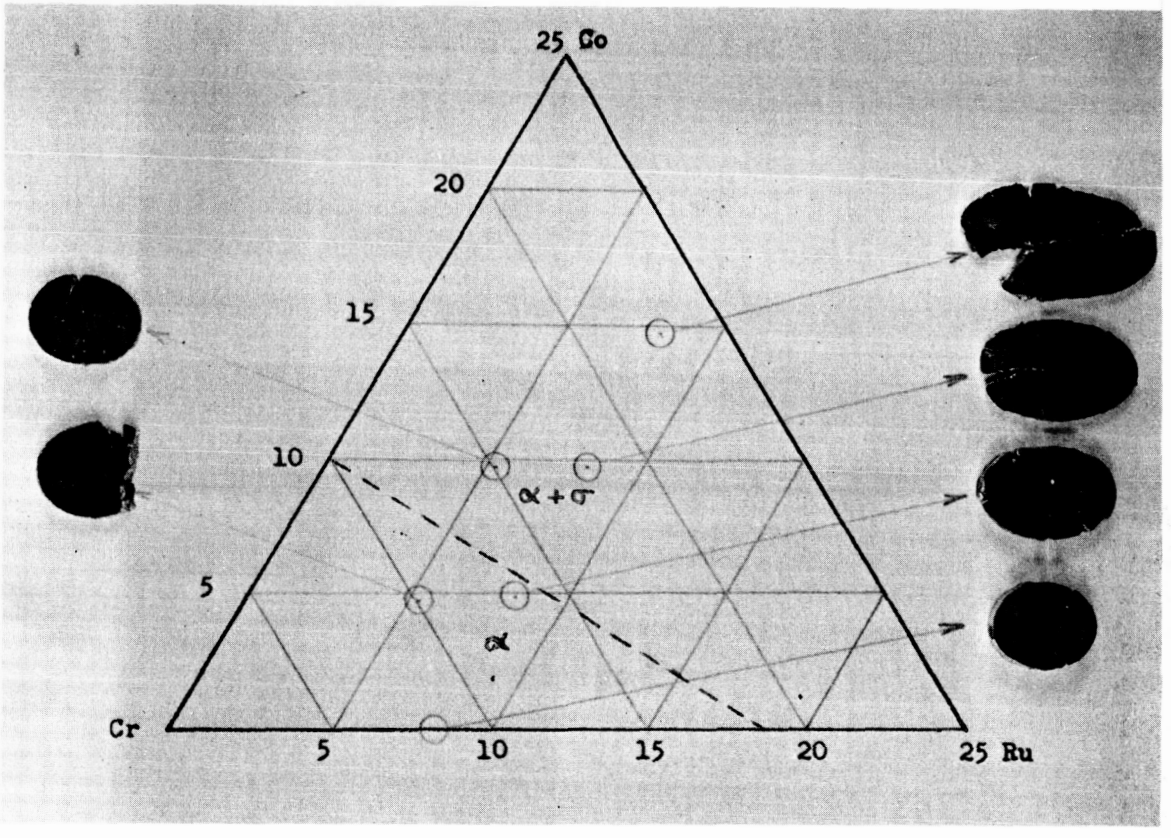

Figure 6. Cold workability of drop cast Cr-Ru-Co alloys with compositions shown in atomic %. Tentative phase boundary at 1650°F.

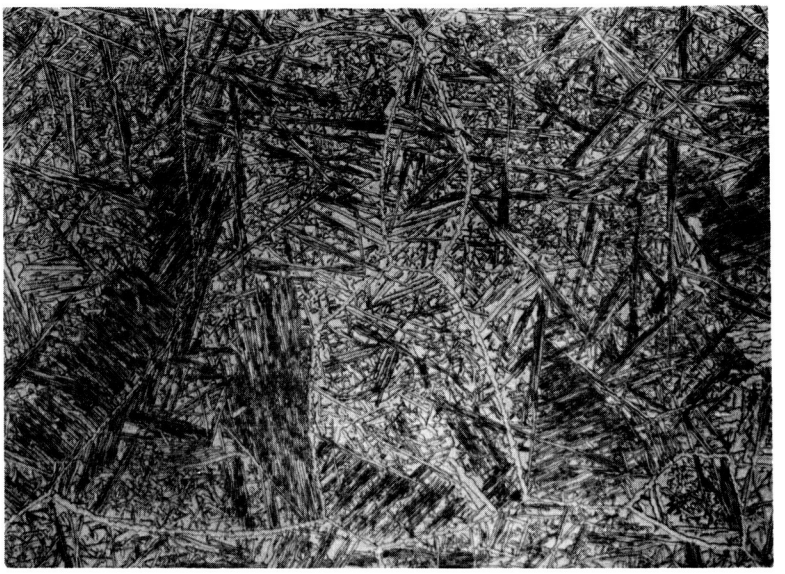

5794 250X

A. Cr-11Re-17.2Co alloy. Approx. 50% sigma

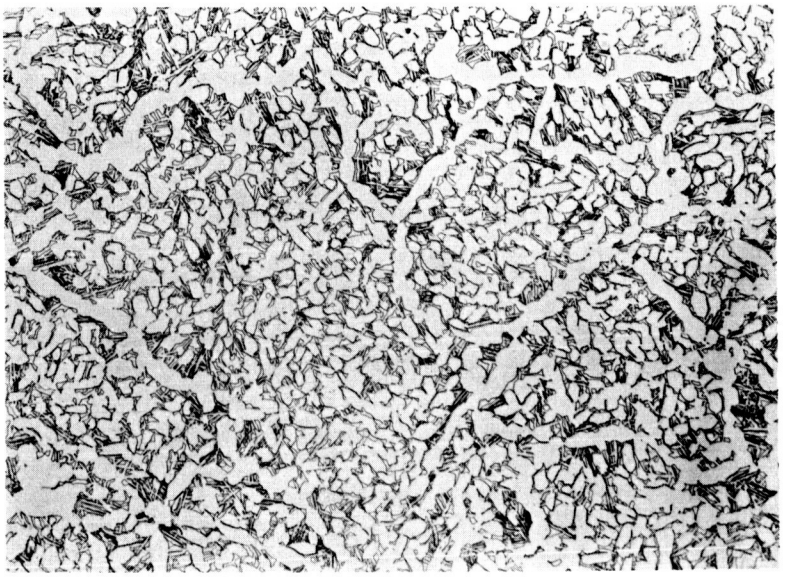

5795 250X

B. Cr-11Re-23.1Co alloy. Approx. 80% sigma

Figure 7. Effect of 100-hour aging at 1650°F on the structure of Cr-Re-Co alloys at indicated atomic concentration. Etched 10% oxalic acid.

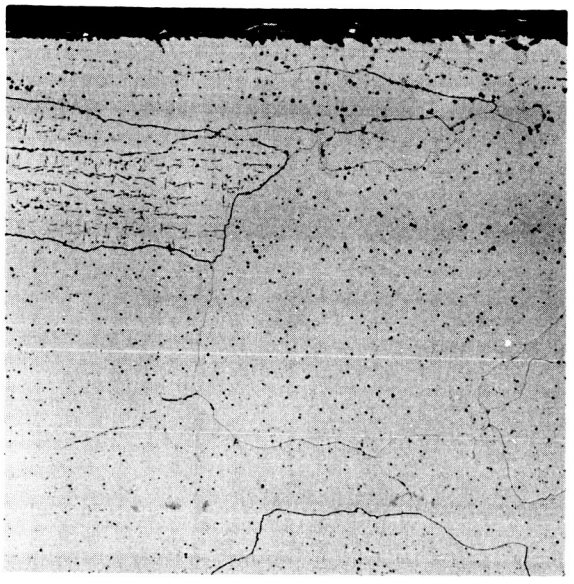

6377 100X

A. Cr-4Re-.1Y, 100 hours at 2100°F

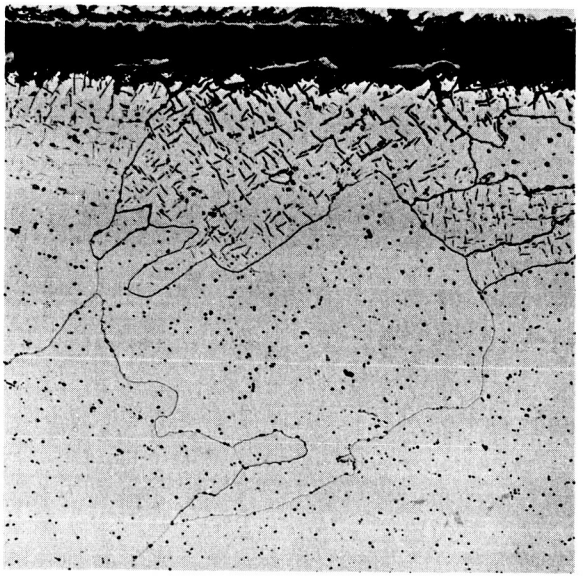

6378 100X

B. Cr-4Re-.1Y, 24 hours at 2400°F

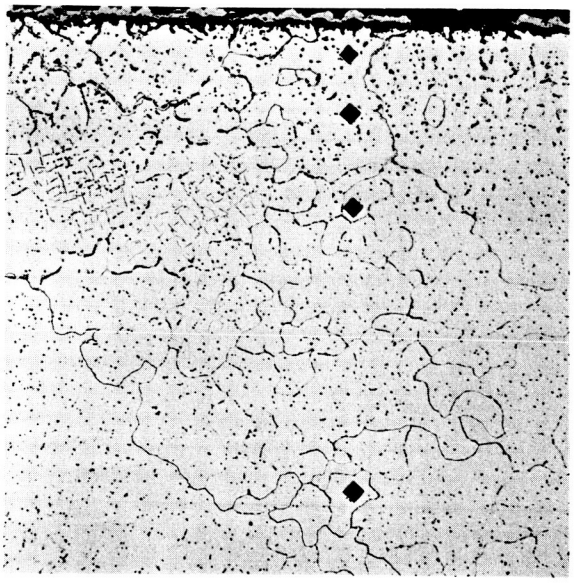

6379 100X

C. Cr-4Re-.5Y, 100 hours at 2100°F

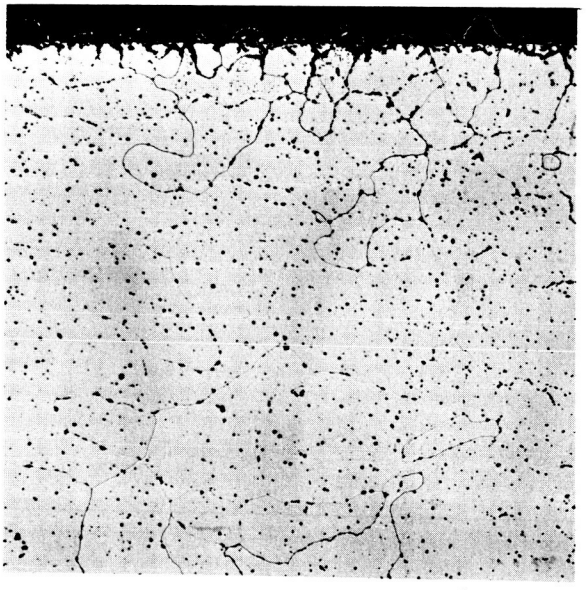

6380 100X

D. Cr-4Re-.5Y, 24 hours at 2400°F

Figure 8. Air oxidation effects on Cr-Re-Y alloys at indicated atomic concentrations. Etched 10% oxalic acid.

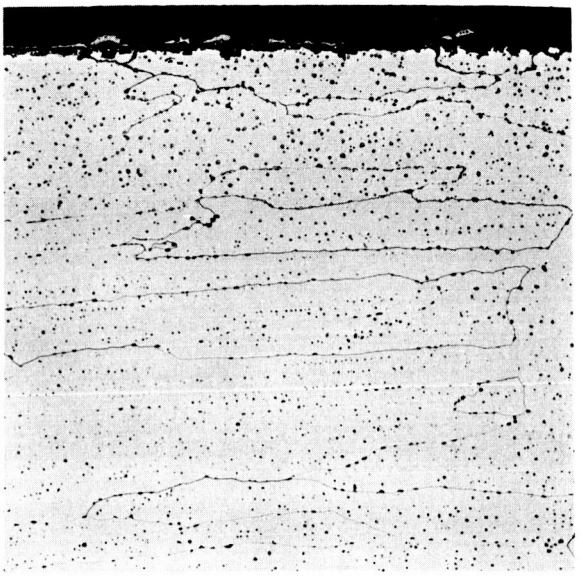

6381 100X

A. Cr-8Re-.5Y, 100 hours at 2100°F

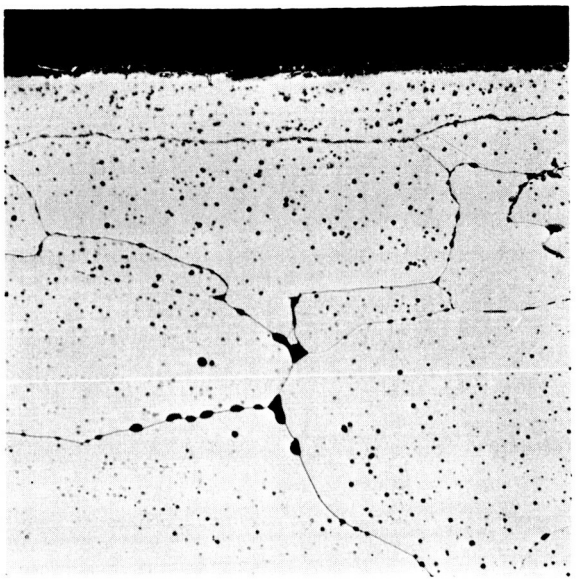

6382 100X

B. Cr-8Re-.5Y, 24 hours at 2400°F

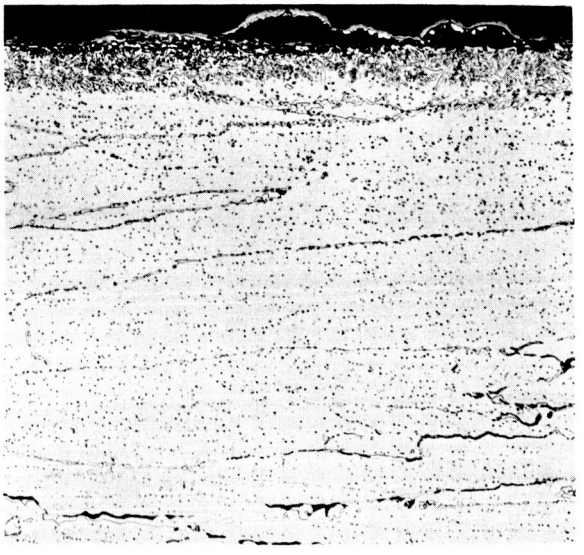

6383 100X

C. Cr-4Ru-.5Y, 24 hours at 2400°F

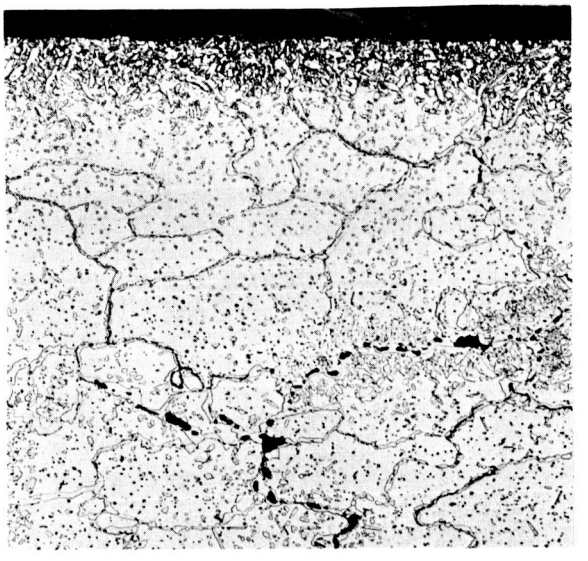

6384 100X

D. Cr-4Co-.5Y, 24 hours at 2400°F

Figure 9. Air oxidation of Cr-.5Y alloys with Re, Ru and Co additions (all atomic %). Etched 10% oxalic acid.

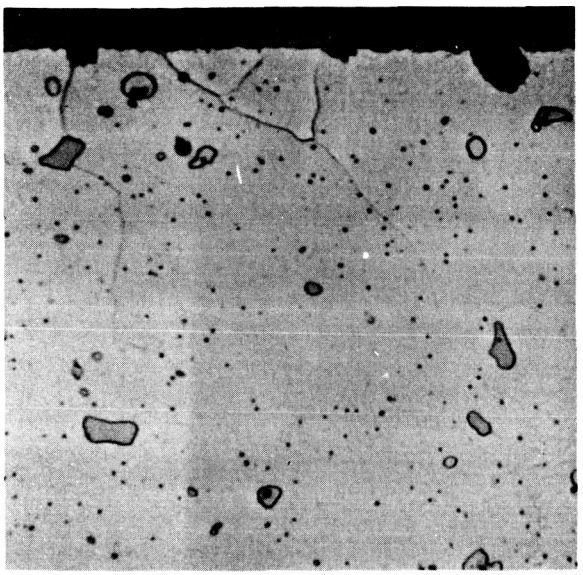

3871 1000X

A. Cr-1Zr-.4C-.1Y at 1500°F

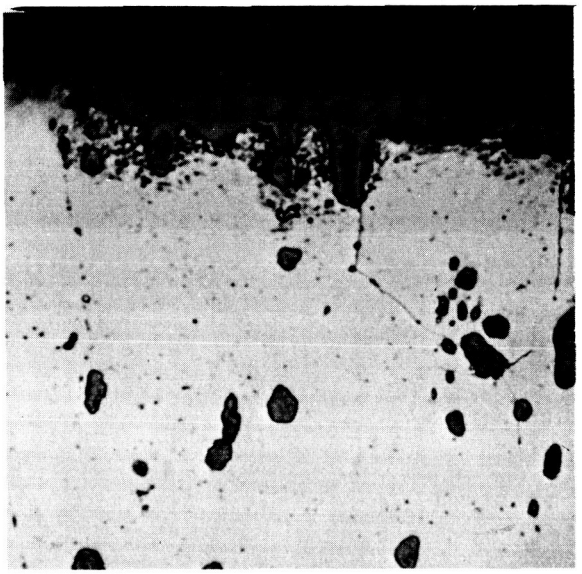

3698 1000X

B. Cr-1Zr-.4C-.1Y at 2100°F

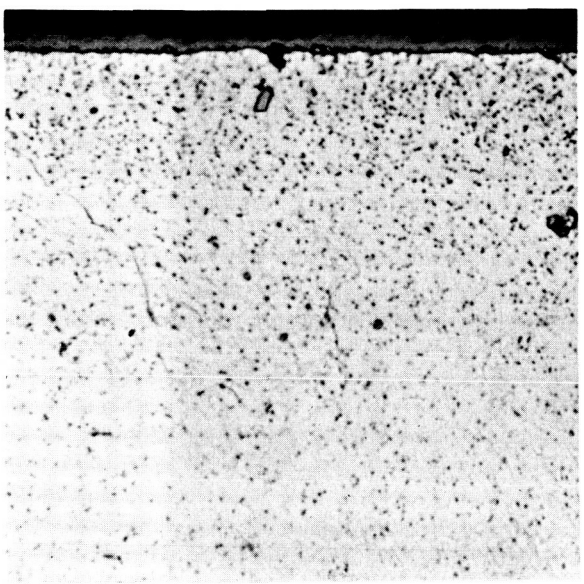

2546 1000X

C. Cr-1Cb.4C-.1Y at 1500°F

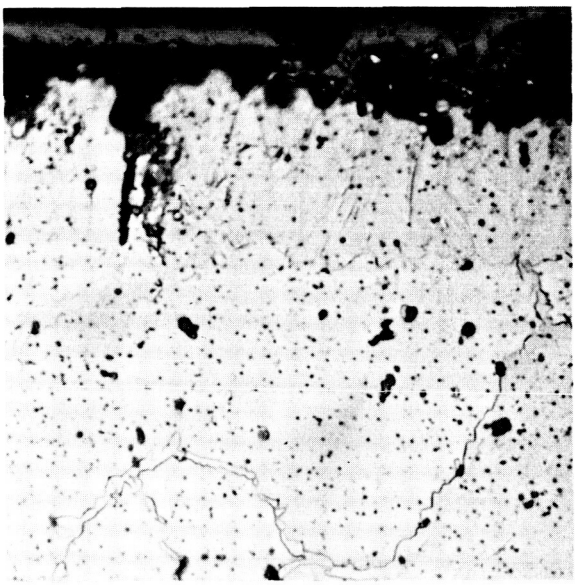

3838 1000X

D. Cr-1Cb-.4C-.1Y at 2100°F

Figure 10. Dilute Cr-Y alloys containing ZrC and CbC dispersions after 100-hour air oxidation at indicated temperatures. Nominal compositions in atomic %. Etched in Kromic acid.

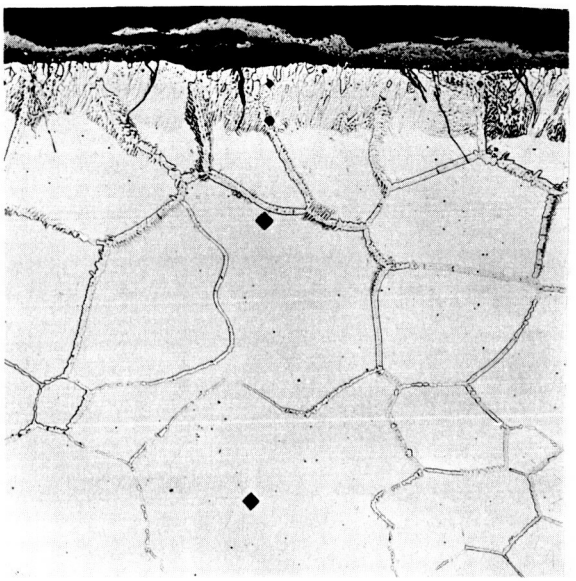

6366 100X

A. Cr-4Mo, 100 hours at 2100°F

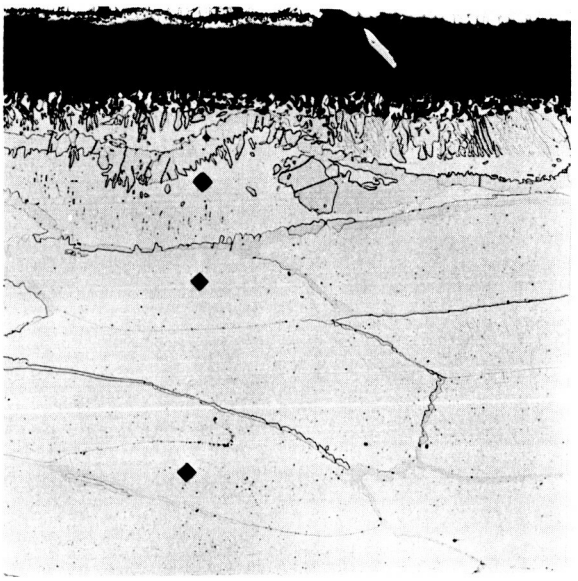

6367 100X

B. Cr-4Mo, 24 hours at 2400°F

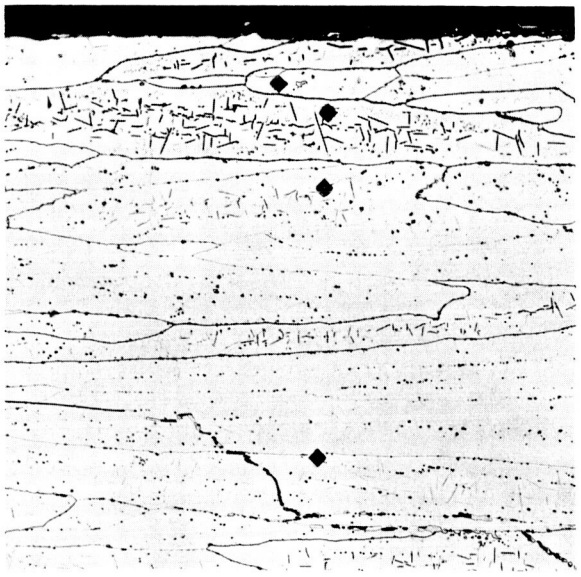

6368 100X

C. Cr-4Mo-.1Y, 100 hours at 2100°F

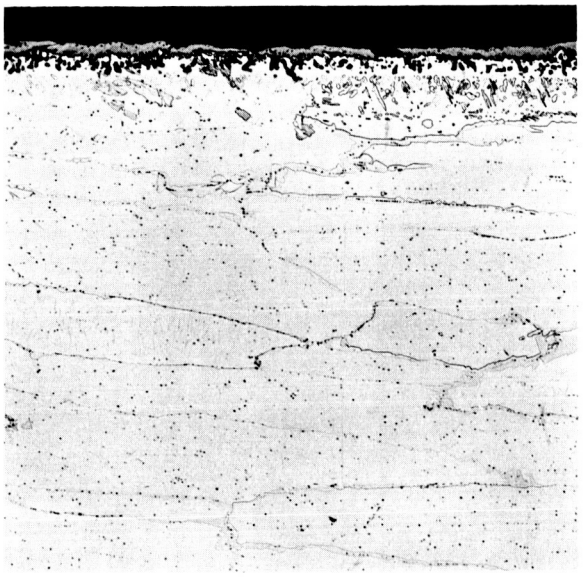

6369 100X

D. Cr-4Mo-.1Y, 24 hours at 2400°F

Figure 11. Effects of 0.1 a/o Y addition on the air oxidation of Cr-4Mo. Etched 10% oxalic acid.

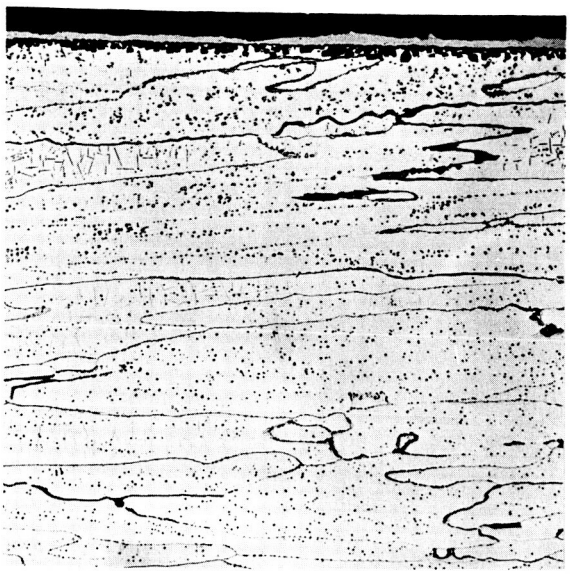

6371 100X

A. Cr-4Mo-.5Y

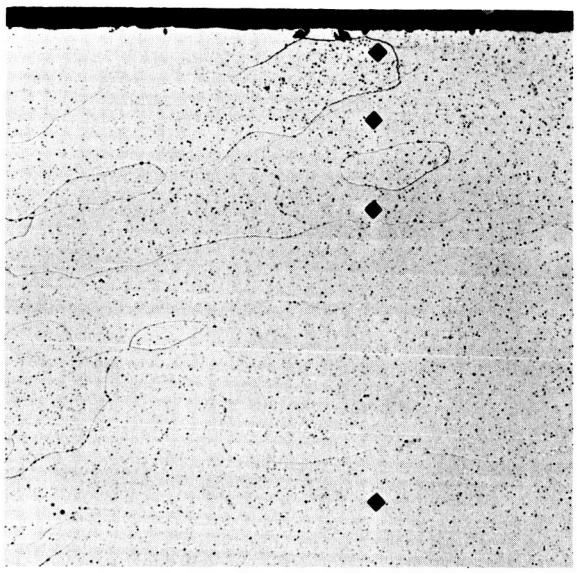

6373 100X

B. Cr-4Mo-.5La

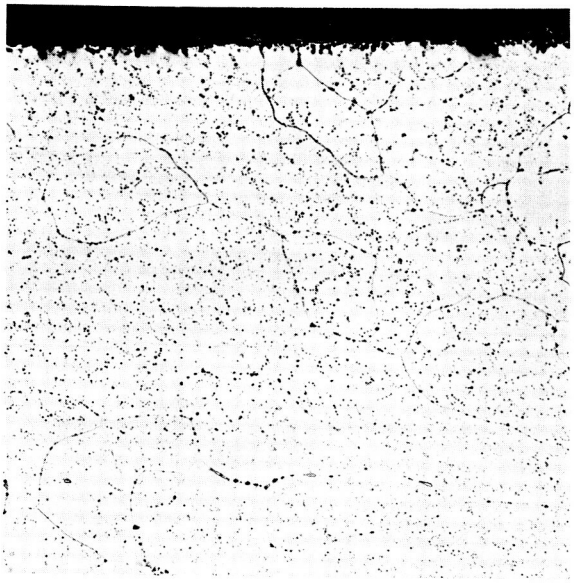

6375 100X

C. Cr-4Mo-.5Pr

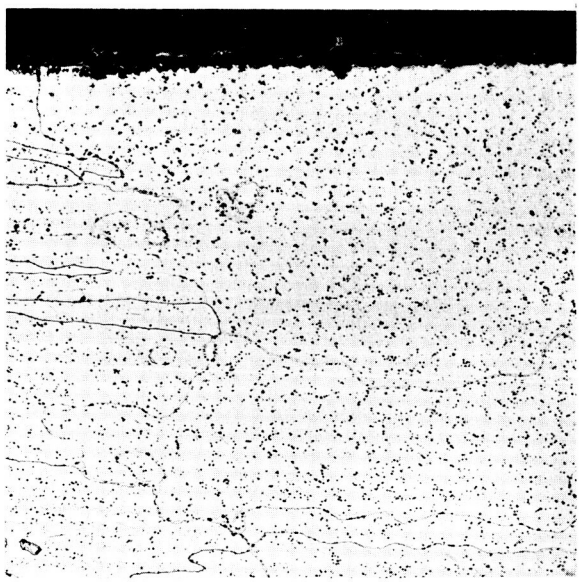

6376 100X

D. Cr-4Mo-.5 Mischmetal

Figure 12. Cr-4Mo alloys with 0.5 atomic % additions of Y, La, Pr and Mischmetal after 24-hour air oxidation at 2400°F. Etched 10% oxalic acid.